Electronic Supplementary Information (ESI) for:

Metal-organic frameworks based on octafluorobiphenyl-4,4'-dicarboxylate: synthesis, crystal structure, and surface functionality

Anastasia M. Cheplakova[1,2], Konstantin A. Kovalenko[1,2*], Denis G. Samsonenko[1,2], Vladimir A. Lazarenko[3], Victor N. Khrustalev[4], Andrey S. Vinogradov[5], Victor M. Karpov[5], Vyacheslav E. Platonov[5], Vladimir P. Fedin[1,2*]

[1] *Nikolaev Institute of Inorganic Chemistry SB RAS, 3 Akad. Lavrentiev Av., 630090 Novosibirsk, Russian Federation.*

[2] *Novosibirsk State University, 2 Pirogova Street, 630090 Novosibirsk, Russian Federation*

[3] *National Research Center «Kurchatov Institute», Acad. Kurchatov Sq. 1, Moscow 123182, Russian Federation*

[4] *Peoples' Friendship University of Russia (RUDN University), Miklukho-Maklay St. 6, Moscow 117198, Russian Federation*

[5] *N.N. Vorozhtsov Novosibirsk Institute of Organic Chemistry SB RAS, 9 Acad. Lavrentiev Av., 630090 Novosibirsk, Russian Federation*

Contents:

* Corresponding author
E-mail: k.a.kovalenko@niic.nsc.ru, cluster@niic.nsc.ru; Fax: +7 (383) 330 9489; Tel: +7 (383) 330 9490

Single crystals of 1

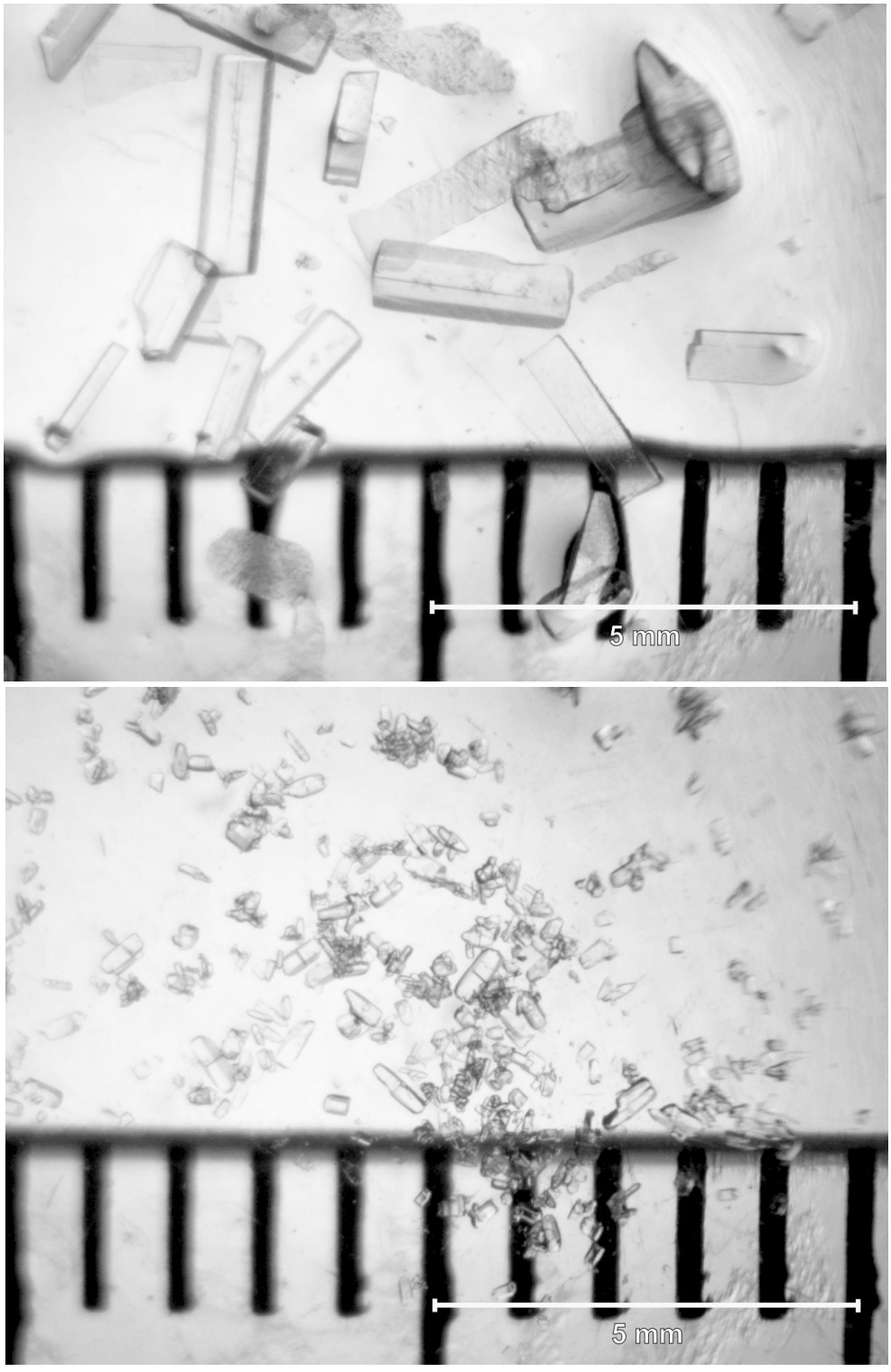

Fig. S1. Single crystals of **1** obtained: a) without additives of acetamide; b) with the presence of acetamide.

Single crystal X-ray structures of 1-6

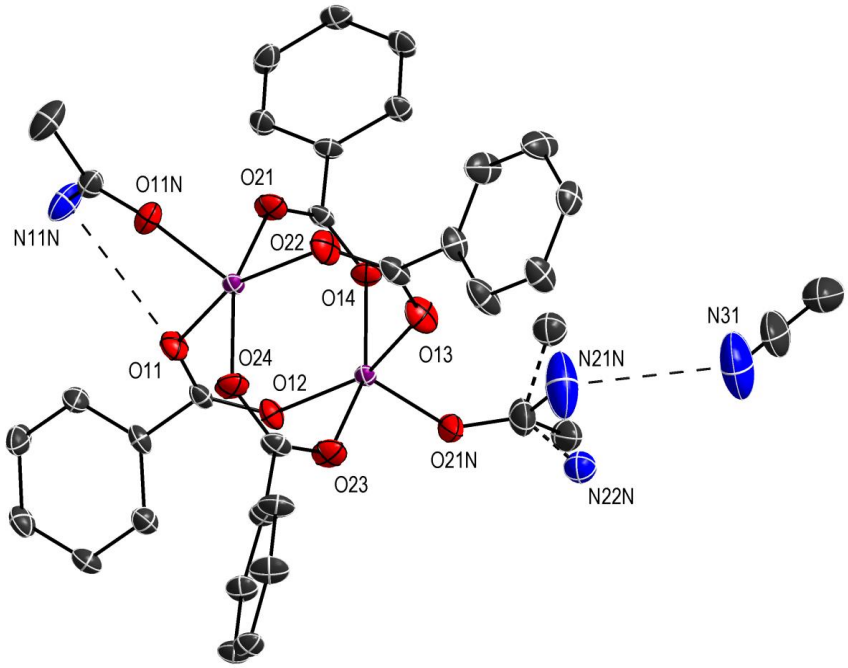

Fig. S2. Coordination environment of Zn(II) cations in the structure **1** (50% probability ellipsoids). Fluorine and hydrogen atoms are omitted for clarity. The alternative orientation of disordered acetamide ligand and hydrogen bonds are shown with dashed lines.

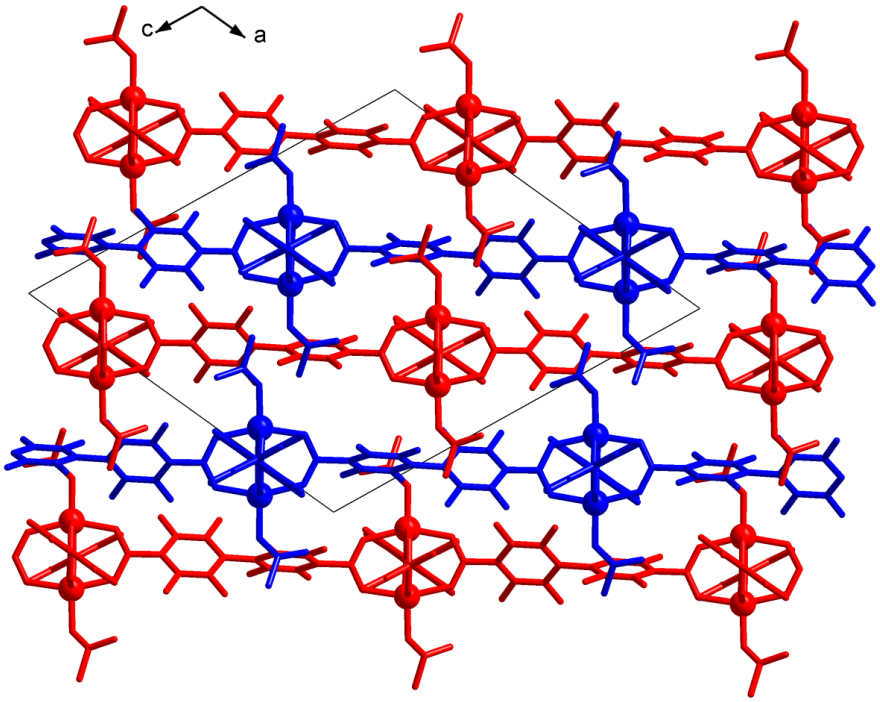

Fig. S3. Packing of the layers in **1**. View along the b axis. Hydrogen atoms and guest molecules of acetonitrile are omitted for clarity.

Table S1. Selected bond lengths and angles for **1**.

Bond	*d*, Å	Bond	*d*, Å
Zn(1)-O(11)	2.057(2)	Zn(2)-O(12)	2.033(2)
Zn(1)-O(14)#1	2.049(2)	Zn(2)-O(13)#1	2.051(2)
Zn(1)-O(21)	2.022(2)	Zn(2)-O(22)	2.038(2)
Zn(1)-O(24)#2	2.036(2)	Zn(2)-O(23)#2	2.046(2)
Zn(1)-O(11N)	1.961(2)	Zn(2)-O(21N)	1.943(2)
Angle	ω, deg.	Angle	ω, deg.
O(14)#1-Zn(1)-O(11)	159.06(10)	O(12)-Zn(2)-O(13)#1	156.02(10)
O(21)-Zn(1)-O(11)	88.73(9)	O(12)-Zn(2)-O(22)	88.64(9)
O(21)-Zn(1)-O(14)#1	88.83(10)	O(12)-Zn(2)-O(23)#2	86.64(9)
O(21)-Zn(1)-O(24)#2	157.10(10)	O(22)-Zn(2)-O(13)#1	89.36(10)
O(24)#2-Zn(1)-O(11)	87.01(10)	O(22)-Zn(2)-O(23)#2	157.81(10)
O(24)#2-Zn(1)-O(14)#1	87.18(10)	O(23)#2-Zn(2)-O(13)#1	86.26(10)
O(11N)-Zn(1)-O(11)	100.91(9)	O(21N)-Zn(2)-O(12)	99.45(10)
O(11N)-Zn(1)-O(14)#1	100.03(10)	O(21N)-Zn(2)-O(13)#1	104.53(11)
O(11N)-Zn(1)-O(21)	97.33(9)	O(21N)-Zn(2)-O(22)	95.93(10)
O(11N)-Zn(1)-O(24)#2	105.57(10)	O(21N)-Zn(2)-O(23)#2	106.23(11)

Symmetry transformations used to generate equivalent atoms:

#1 $x + ½, −y + 3/2, z − ½$; #2 $x, y + 1, z$.

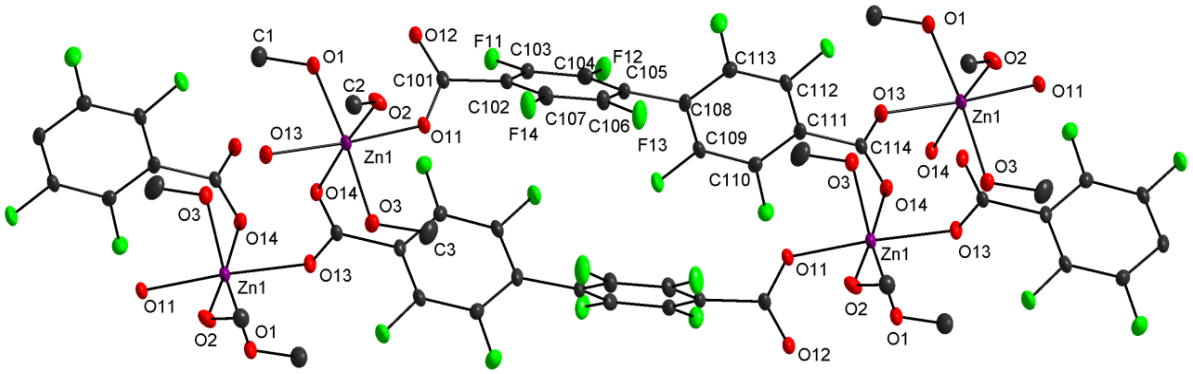

Fig. S4. Coordination environment of Zn(II) cations in the structure **2** (50% probability ellipsoids). Hydrogen atoms are omitted for clarity.

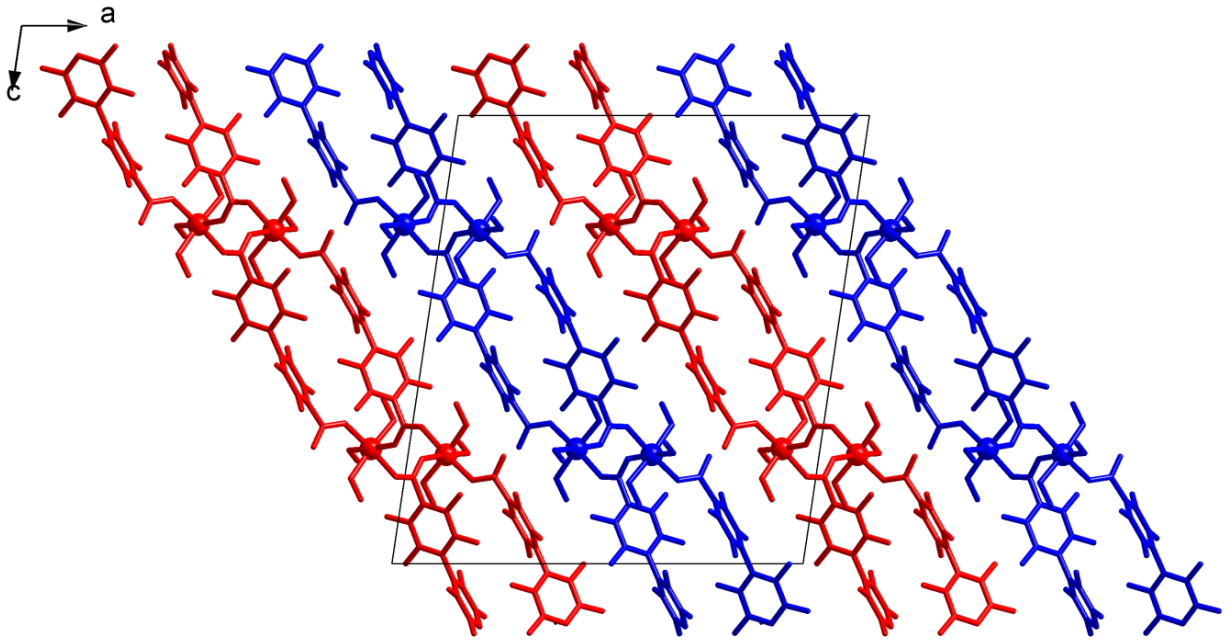

Fig. S5. Packing of the polymeric layers in the structure **2** (projection on *ac* plane). Hydrogen atoms are omitted for clarity.

Table S2. Selected bond lengths and angles for **2**.

Bond	*d*, Å	Bond	*d*, Å
Zn(1)-O(1)	2.0745(11)	Zn(1)-O(11)	2.0324(10)
Zn(1)-O(2)	2.1165(12)	Zn(1)-O(13)#1	2.0711(11)
Zn(1)-O(3)	2.1038(11)	Zn(1)-O(14)#2	2.1674(11)
Angle	ω, deg.	Angle	ω, deg.
O(1)-Zn(1)-O(2)	93.04(5)	O(11)-Zn(1)-O(3)	93.70(4)
O(1)-Zn(1)-O(3)	175.26(4)	O(11)-Zn(1)-O(13)#1	175.95(4)
O(1)-Zn(1)-O(14)#2	91.88(4)	O(11)-Zn(1)-O(14)#2	94.51(4)
O(2)-Zn(1)-O(14)#2	175.08(4)	O(13)#1-Zn(1)-O(1)	85.83(4)
O(3)-Zn(1)-O(2)	88.34(5)	O(13)#1-Zn(1)-O(2)	92.45(5)
O(3)-Zn(1)-O(14)#2	86.77(4)	O(13)#1-Zn(1)-O(3)	89.58(4)
O(11)-Zn(1)-O(1)	90.93(4)	O(13)#1-Zn(1)-O(14)#2	88.03(4)
O(11)-Zn(1)-O(2)	85.28(5)		

Symmetry transformations used to generate equivalent atoms:

#1 $x - ½$, y + ½, $z - ½$; #2 $-x + ½$, y, $-z + 1$.

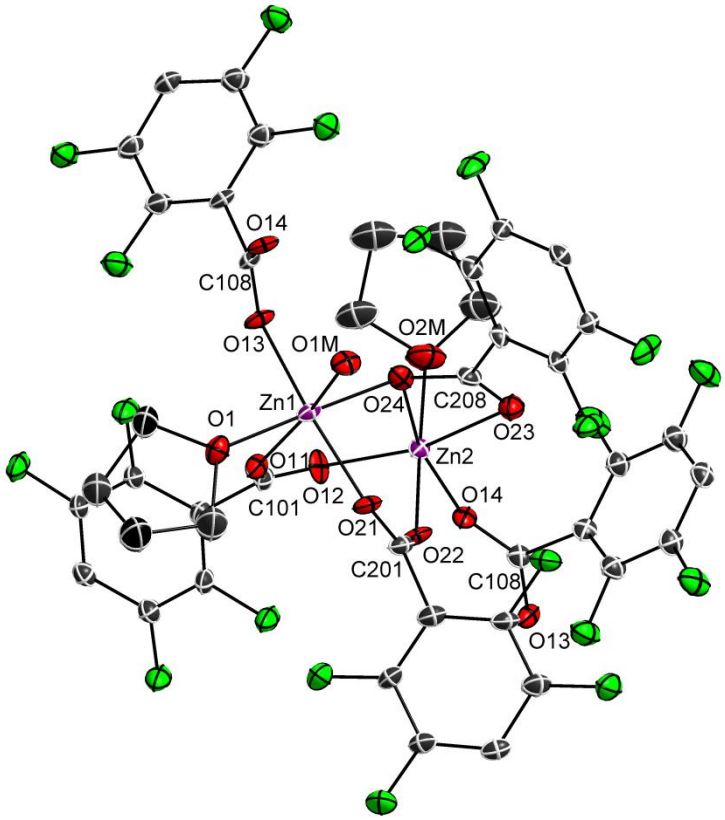

Fig. S6. Coordination environment of Zn(II) cations in the structure **3** (50% probability ellipsoids). Hydrogen atoms are omitted for clarity.

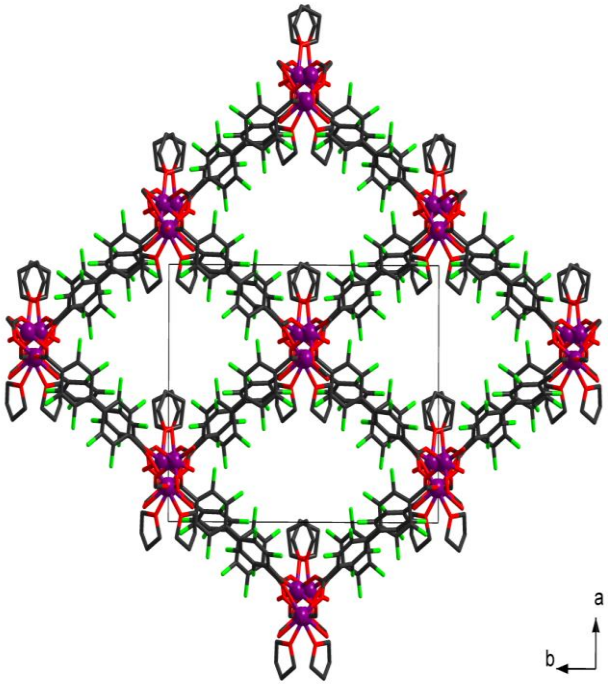

Fig. S7. Structure of metal-organic framework **3** (projection on *ab* plane). Hydrogen atoms are omitted for clarity.

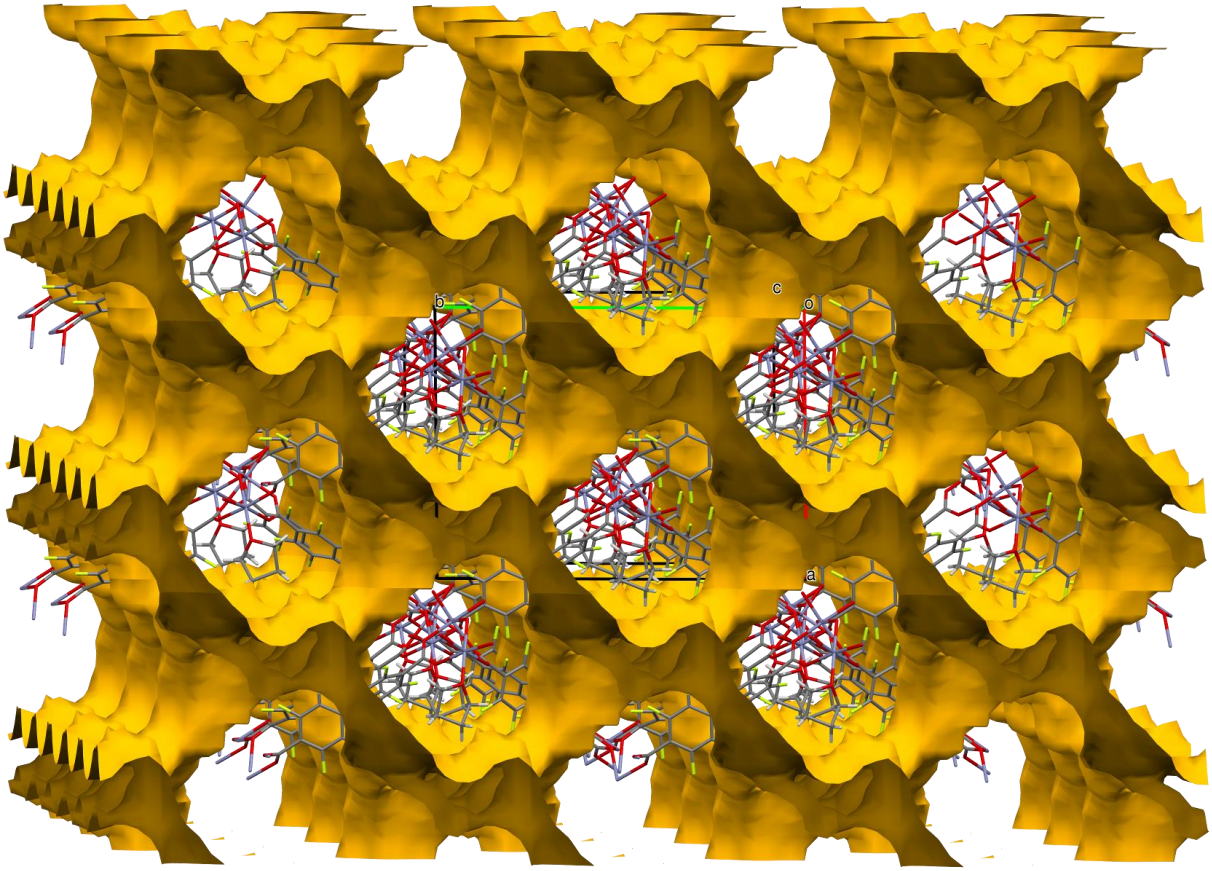

Fig. S8. Representation of the free solvent accessible void volume in the structure **3**.

Table S3. Selected bond lengths and angles for **3**.

Bond	*d*, Å	Bond	*d*, Å
Zn(1)-O(1M)	2.085(9)	Zn(2)-O(2M)	2.068(11)
Zn(1)-O(11)	2.096(9)	Zn(2)-O(12)	1.995(9)
Zn(1)-O(13)#1	2.062(9)	Zn(2)-O(14)#3	2.017(8)
Zn(1)-O(21)	2.062(9)	Zn(2)-O(22)	2.094(9)
Zn(1)-O(24)#2	2.103(9)	Zn(2)-O(23)#2	2.172(10)
Zn(1)-O(1)	2.116(10)	Zn(2)-O(24)#2	2.207(10)
Angle	ω, deg.	Angle	ω, deg.
O(1M)-Zn(1)-O(11)	170.4(4)	O(2M)-Zn(2)-O(22)	175.6(4)
O(1M)-Zn(1)-O(24)#2	92.4(4)	O(2M)-Zn(2)-O(23)#2	88.7(4)
O(1M)-Zn(1)-O(1)	88.1(4)	O(2M)-Zn(2)-O(24)#2	88.9(4)
O(11)-Zn(1)-O(24)#2	97.1(4)	O(12)-Zn(2)-O(2M)	89.5(5)
O(11)-Zn(1)-O(1)	82.4(4)	O(12)-Zn(2)-O(14)#3	92.9(4)
O(13)#1-Zn(1)-O(1M)	93.6(4)	O(12)-Zn(2)-O(22)	93.3(4)
O(13)#1-Zn(1)-O(11)	86.4(3)	O(12)-Zn(2)-O(23)#2	162.4(4)
O(13)#1-Zn(1)-O(24)#2	85.7(4)	O(12)-Zn(2)-O(24)#2	102.7(4)
O(13)#1-Zn(1)-O(1)	95.5(4)	O(14)#3-Zn(2)-O(2M)	96.2(4)
O(21)-Zn(1)-O(1M)	89.5(4)	O(14)#3-Zn(2)-O(22)	87.0(4)
O(21)-Zn(1)-O(11)	91.6(4)	O(14)#3-Zn(2)-O(23)#2	104.7(4)
O(21)-Zn(1)-O(13)#1	172.9(4)	O(14)#3-Zn(2)-O(24)#2	163.6(4)
O(21)-Zn(1)-O(24)#2	87.8(4)	O(22)-Zn(2)-O(23)#2	87.6(4)
O(21)-Zn(1)-O(1)	91.0(4)	O(22)-Zn(2)-O(24)#2	87.1(3)
O(24)#2-Zn(1)-O(1)	178.7(4)	O(23)#2-Zn(2)-O(24)#2	59.8(4)

Symmetry transformations used to generate equivalent atoms:

#1 $x - ½, -y + 3/2, z - ½$; #2 $x - ½, -y + ½, z - ½$; #3 $x - ½, y - ½, z$.

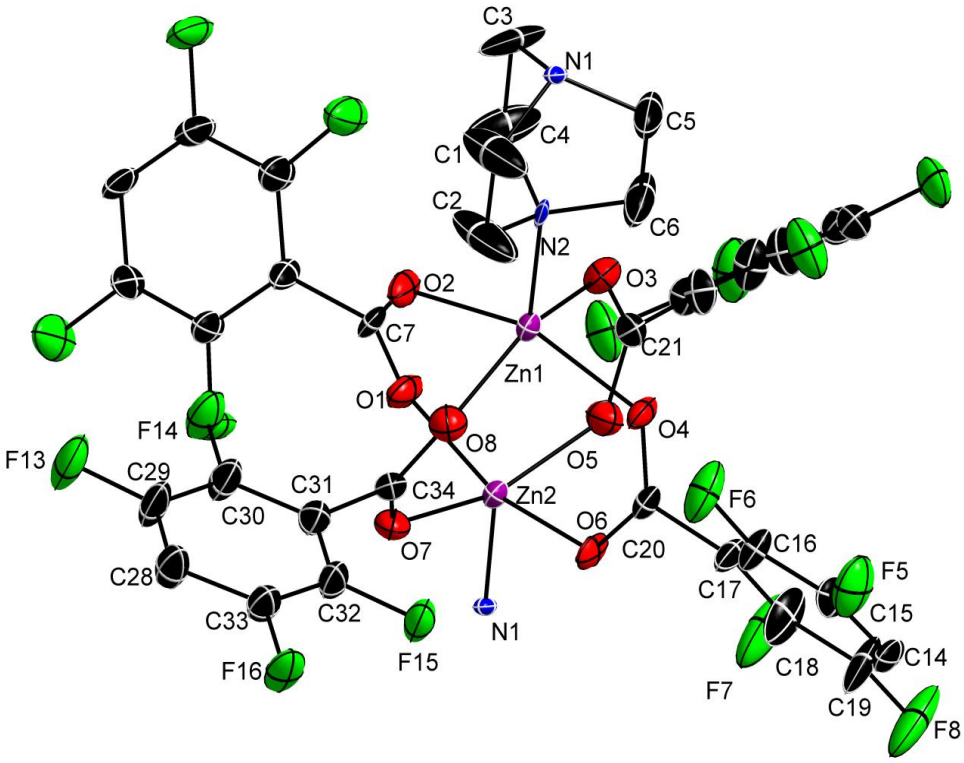

Fig. S9. Coordination environment of Zn(II) cations in the structure **4** (50% probability ellipsoids). Hydrogen atoms are omitted for clarity.

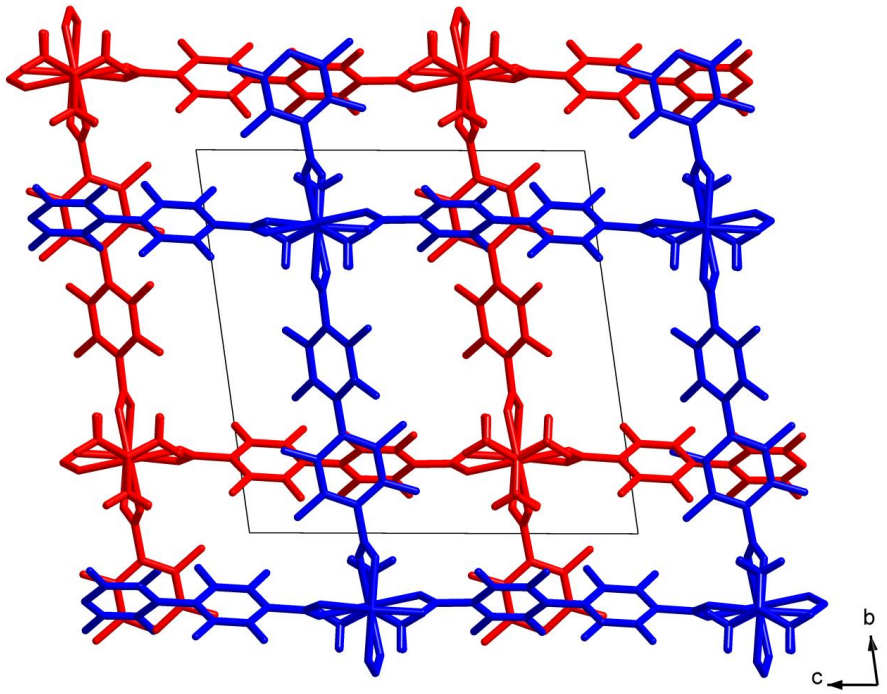

Fig. S10. Crystal packing of the metal-organic frameworks in the structure **4** (projection on *bc* plane).

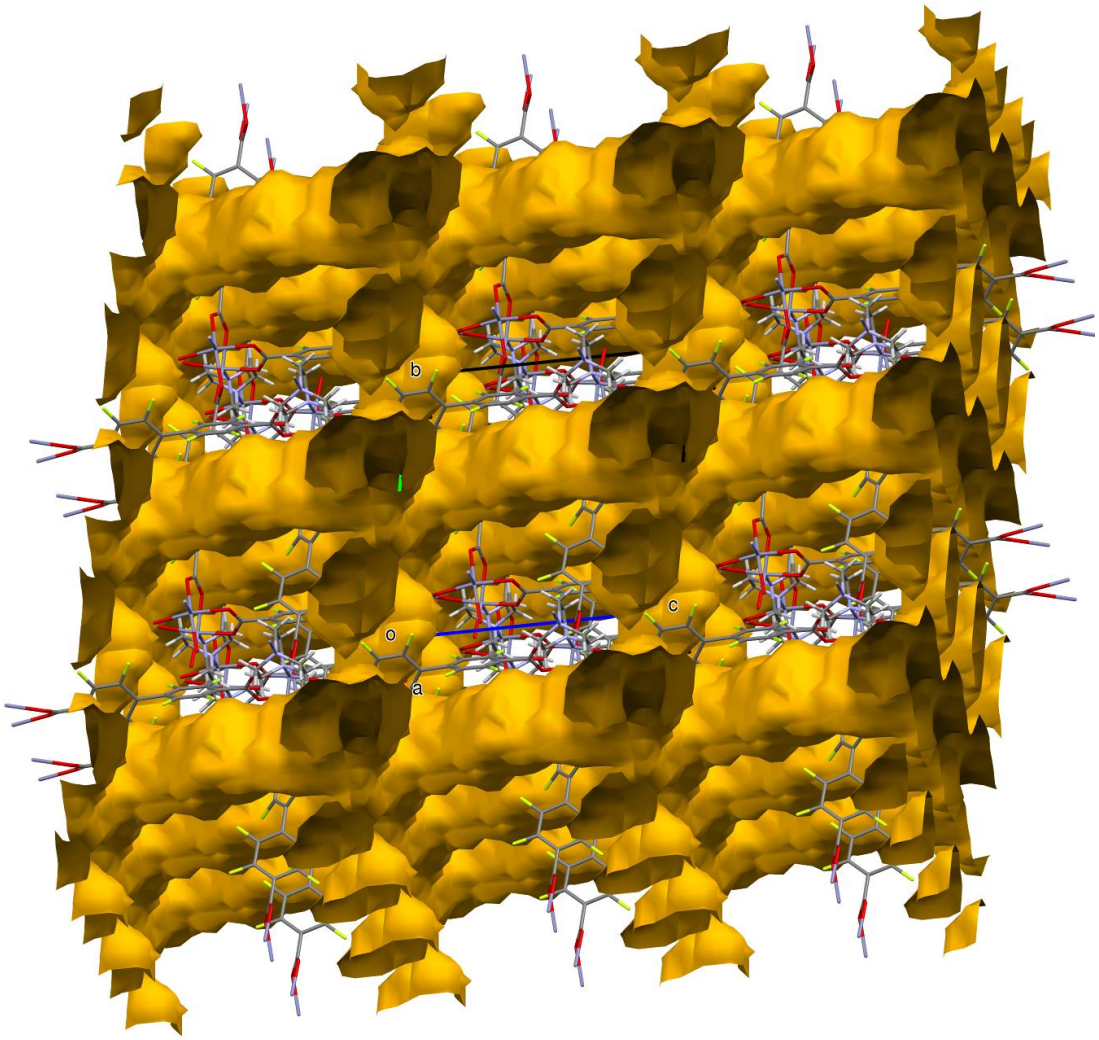

Fig. S11. Representation of the free solvent accessible void volume in the structure **4**.

Table S4. Selected bond lengths and angles for **4**.

Bond	*d*, Å	Bond	*d*, Å
Zn(1)-O(1)#1	2.061(5)	Zn(2)-O(3)	2.056(6)
Zn(1)-O(5)	2.048(6)	Zn(2)-O(4)	2.044(4)
Zn(1)-O(6)	2.062(4)	Zn(2)-O(8)#2	2.085(6)
Zn(1)-O(7)#2	2.056(6)	Zn(2)-N(2)#3	2.059(6)
Zn(1)-N(1)	2.064(6)		
Angle	ω, deg.	Angle	ω, deg.
O(1)#1-Zn(1)-O(6)	156.8(2)	O(2)#1-Zn(2)-O(8)#2	85.7(2)
O(1)#1-Zn(1)-N(1)	102.5(2)	O(3)-Zn(2)-O(2)#1	89.9(2)
O(5)-Zn(1)-O(1)#1	88.3(2)	O(3)-Zn(2)-O(8)#2	157.4(2)
O(5)-Zn(1)-O(6)	87.7(2)	O(3)-Zn(2)-N(2)#3	101.6(2)
O(5)-Zn(1)-O(7)#2	157.0(2)	O(4)-Zn(2)-O(2)#1	156.1(2)
O(5)-Zn(1)-N(1)	99.3(2)	O(4)-Zn(2)-O(3)	88.1(2)
O(6)-Zn(1)-N(1)	100.7(2)	O(4)-Zn(2)-O(8)#2	87.0(2)
O(7)#2-Zn(1)-O(1)#1	87.0(2)	O(4)-Zn(2)-N(2)#3	103.6(2)
O(7)#2-Zn(1)-O(6)	87.8(2)	N(2)#3-Zn(2)-O(2)#1	100.2(2)
O(7)#2-Zn(1)-N(1)	103.8(2)	N(2)#3-Zn(2)-O(8)#2	101.1(2)

Symmetry transformations used to generate equivalent atoms:

#1 *x*, *y*, *z* − 1; #2 *x*, *y* − 1, *z*; #3 *x* − 1, *y*, *z*.

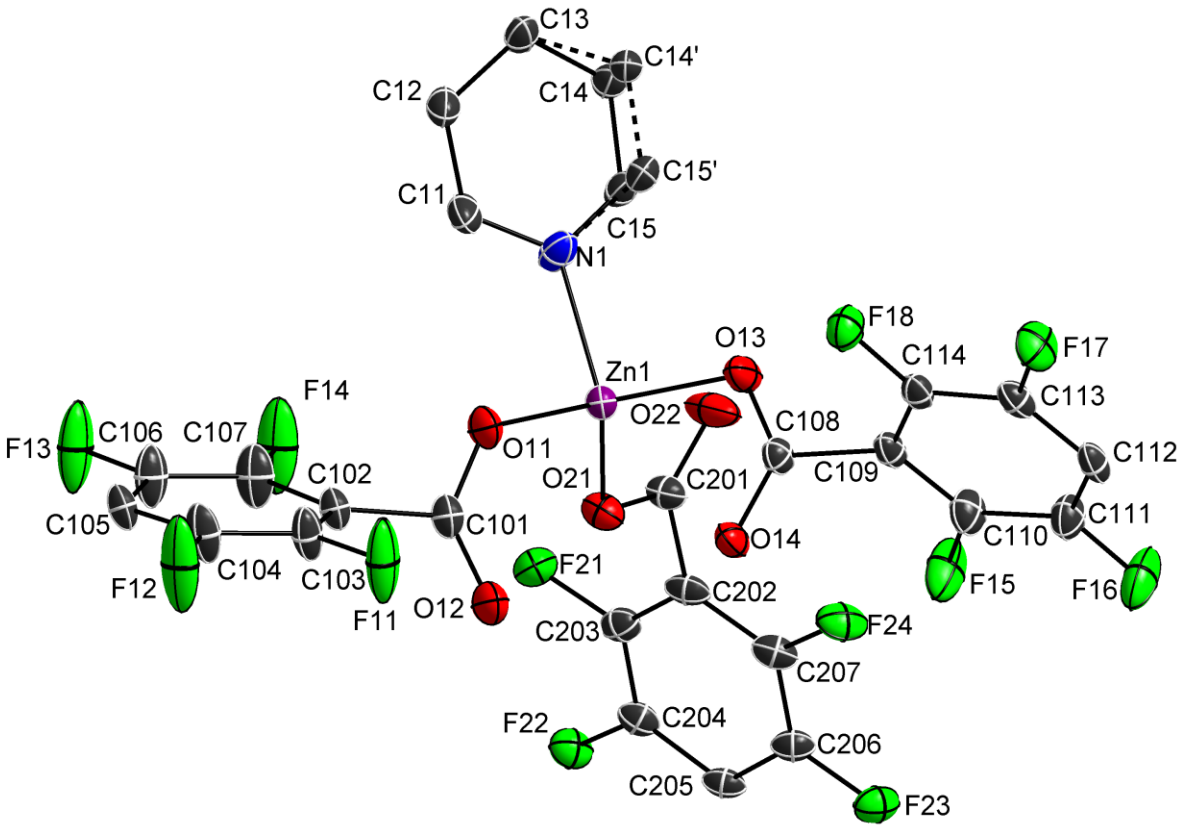

Fig. S12. Coordination environment of Zn(II) cation in the structure **5** (50% probability ellipsoids). Hydrogen atoms are omitted for clarity.

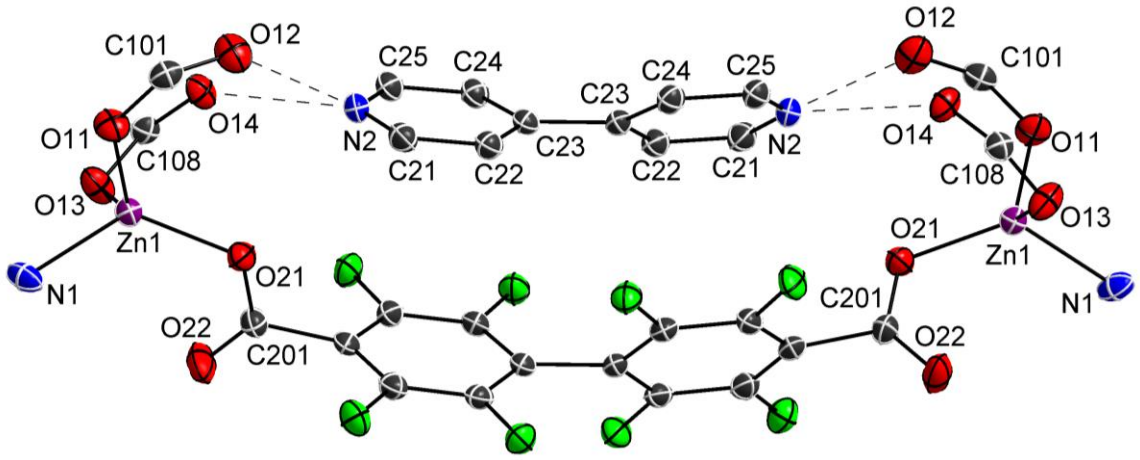

Fig. S13. Coordination environment of Zn(II) cation in the structure **5** (50% probability ellipsoids). Hydrogen atoms are omitted for clarity.

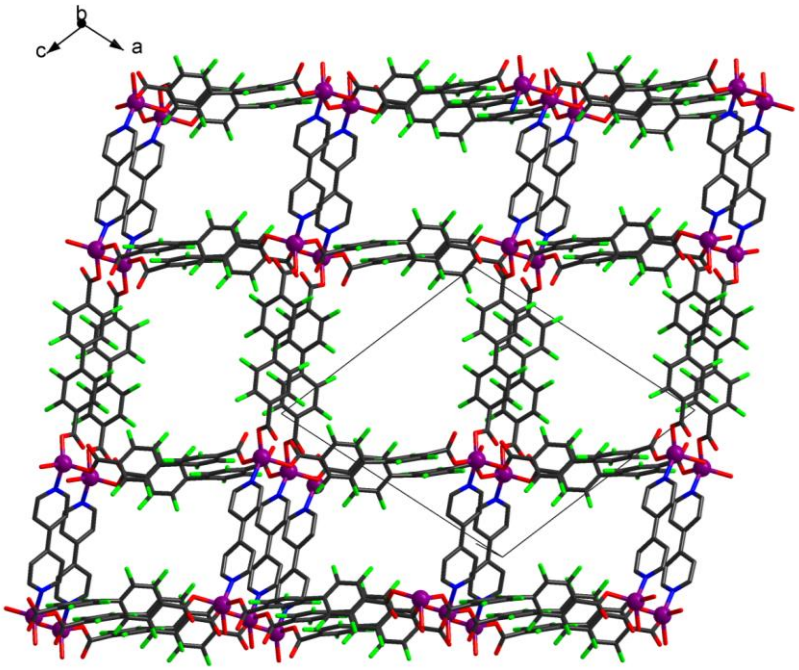

Fig. S14. The structure of metal-organic framework **5**. Hydrogen atoms are omitted for clarity.

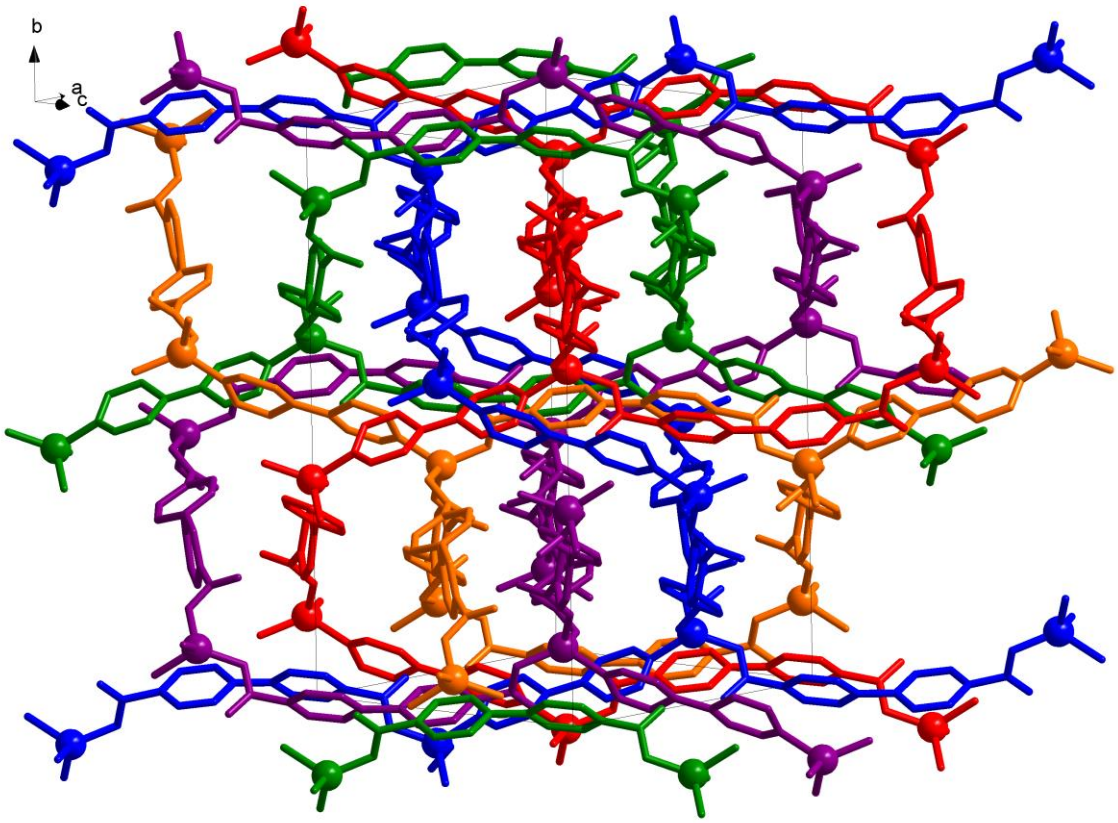

Fig. S15. Crystal packing of the metal-organic frameworks in the structure **5**. H_2bpy^{2+} cations are omitted for clarity.

Table S5. Selected bond lengths and angles for **5**.

Bond	*d*, Å	Bond	*d*, Å
Zn(1)-O(11)	1.9497(17)	Zn(1)-O(21)	1.9341(17)
Zn(1)-O(13)#1	1.9716(17)	Zn(1)-N(1)	2.025(2)
Angle	ω, deg.	Angle	ω, deg.
O(11)-Zn(1)-O(13)#1	118.19(8)	O(21)-Zn(1)-O(11)	109.55(8)
O(11)-Zn(1)-N(1)	93.67(8)	O(21)-Zn(1)-O(13)#1	112.83(8)
O(13)#1-Zn(1)-N(1)	98.51(8)	O(21)-Zn(1)-N(1)	123.17(9)

Symmetry transformations used to generate equivalent atoms: #1 $x - ½, -y + ½, z + ½$.

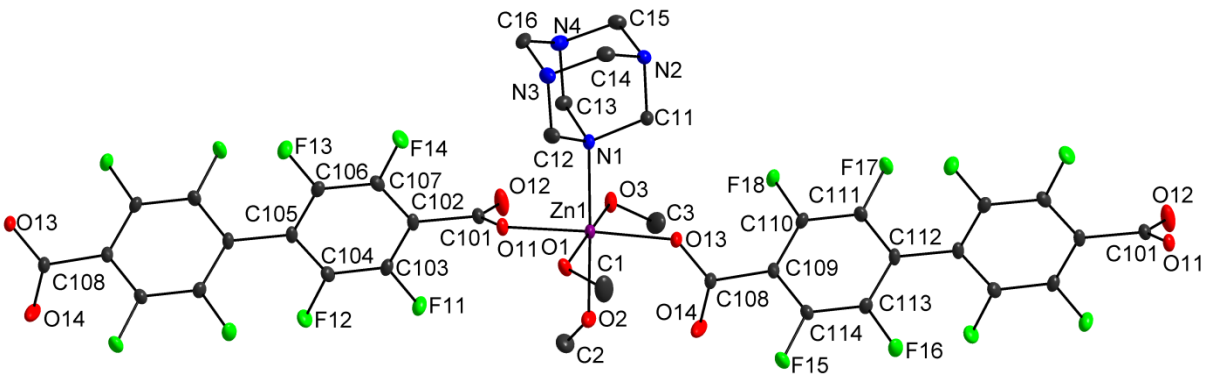

Fig. S16. Coordination environment of Zn(II) cation in the structure **6** (50% probability ellipsoids). Hydrogen atoms are omitted for clarity.

Table S6. Selected bond lengths and angles for **6**.

Bond	*d*, Å	Bond	*d*, Å
Zn(1)-O(1)	2.1189(10)	Zn(1)-N(1)	2.1854(12)
Zn(1)-O(2)	2.1476(11)	Zn(1)-O(11)	2.0770(10)
Zn(1)-O(3)	2.1361(11)	Zn(1)-O(13)#1	2.0761(10)
Angle	ω, deg.	Angle	ω, deg.
O(1)-Zn(1)-O(2)	85.38(5)	O(11)-Zn(1)-O(3)	90.69(4)
O(1)-Zn(1)-O(3)	174.36(4)	O(11)-Zn(1)-N(1)	90.44(4)
O(1)-Zn(1)-N(1)	94.75(4)	O(13)#1-Zn(1)-O(1)	90.35(4)
O(2)-Zn(1)-N(1)	178.40(4)	O(13)#1-Zn(1)-O(2)	90.65(4)
O(3)-Zn(1)-O(2)	89.72(4)	O(13)#1-Zn(1)-O(3)	92.50(4)
O(3)-Zn(1)-N(1)	90.08(4)	O(13)#1-Zn(1)-N(1)	90.94(4)
O(11)-Zn(1)-O(1)	86.36(4)	O(13)#1-Zn(1)-O(11)	176.52(4)
O(11)-Zn(1)-O(2)	87.97(4)		

Symmetry transformations used to generate equivalent atoms: #1 $x + 1$, y, $z + 1$.

PXRD, FT-IR spectra, and TGA

Complex **1**

$[Zn_2(CH_3CONH_2)_2(oFBPDC)_2]\cdot 3CH_3CN$

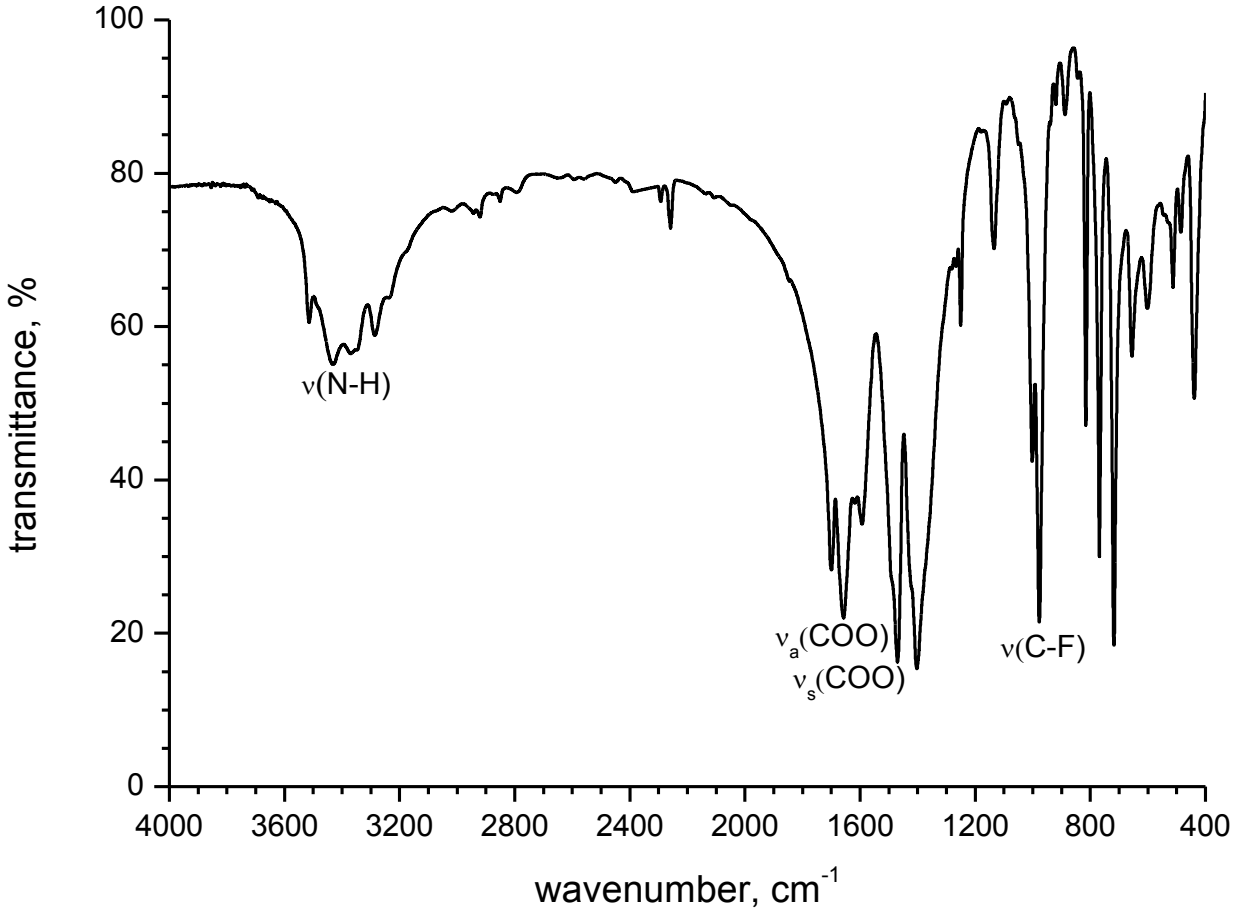

Fig. S17. The FT-IR spectrum of complex **1**.

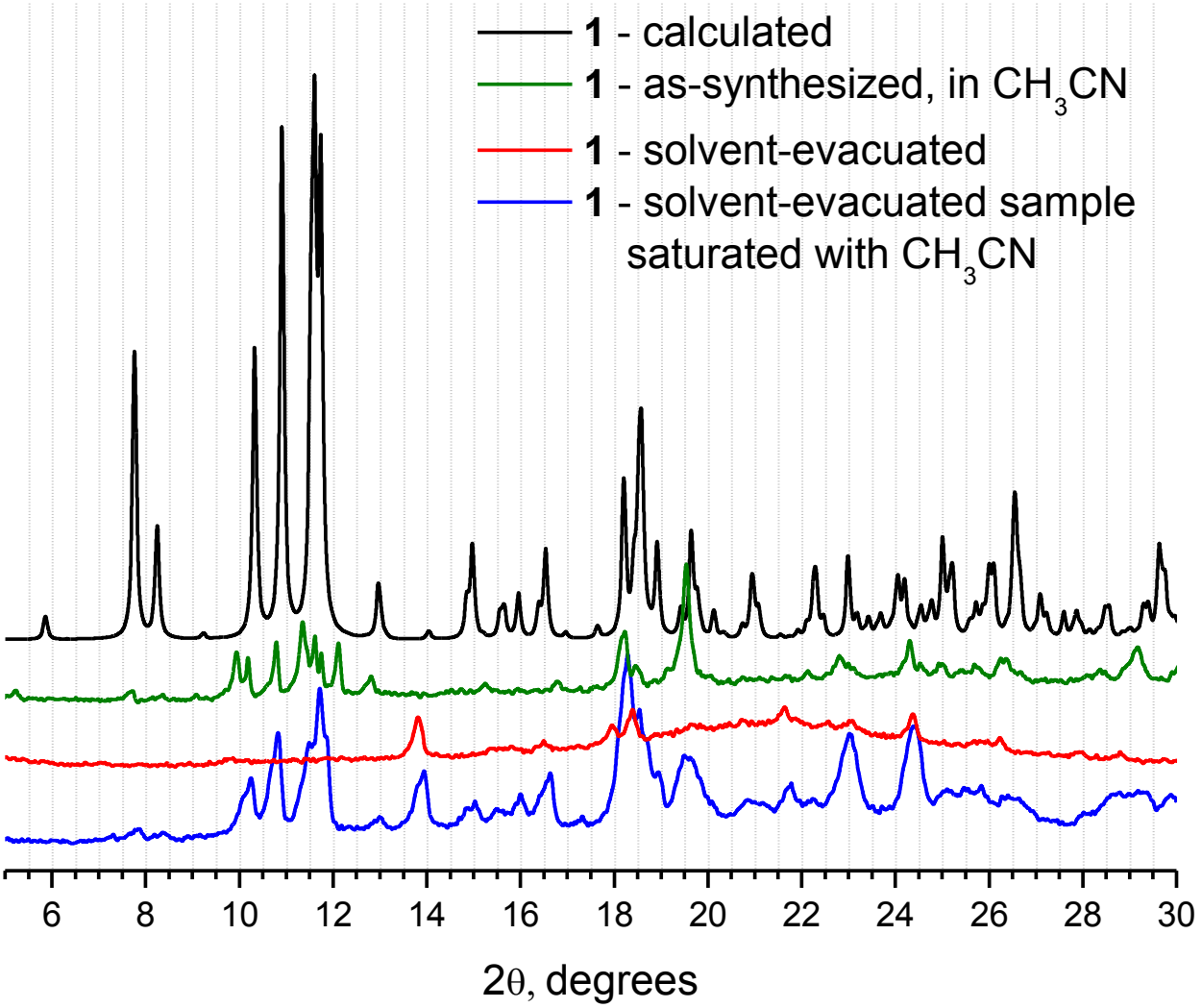

Fig. S18. PXRD patterns of **1**: calculated pattern (black line), the pattern of the as-synthesized sample recordered in CH_3CN (green line), the pattern of the solvent-evacuated sample (red line) and pattern of sample resaturated with CH_3CN (blue line). Green and red lines indicate that the sample loses original crystal structure along with the removal of the solvent and further solvent evacuation. Blue line confirms partial restoration of the crystal structure when soaking in CH_3CN.

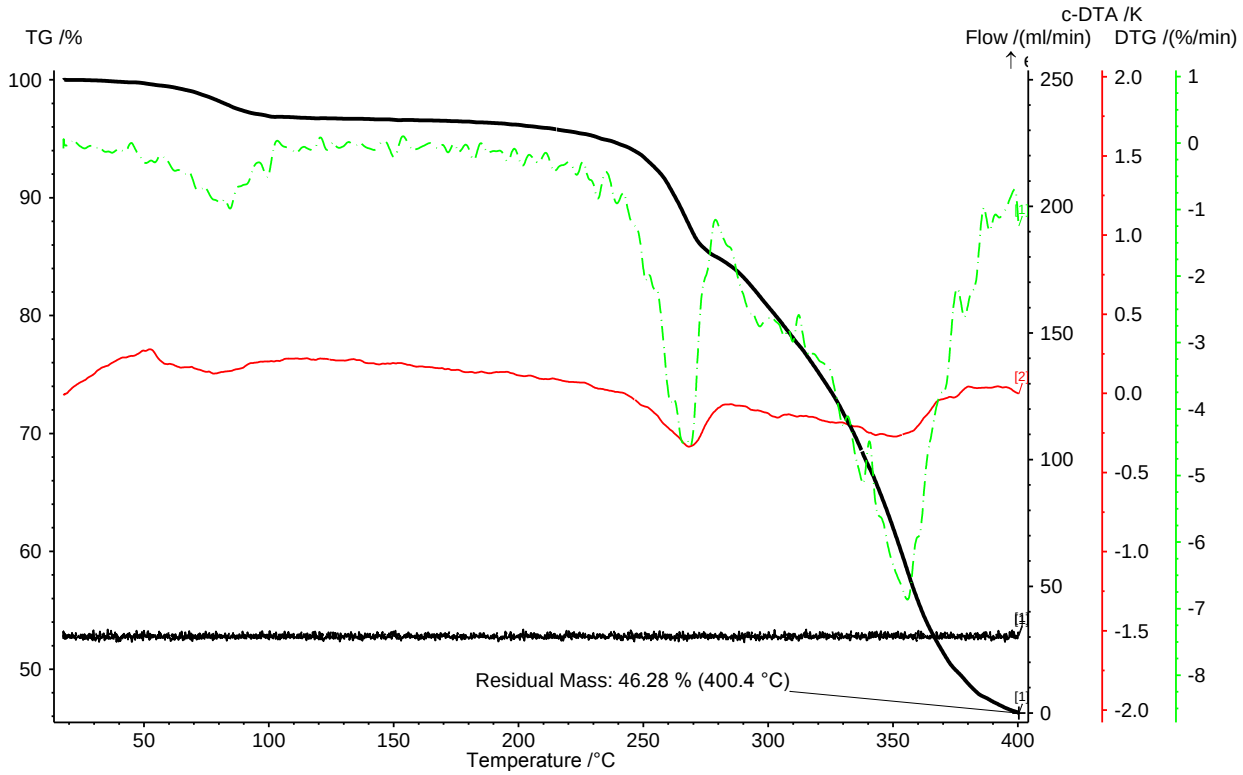

Fig. S19. TG curve of complex **1**.

Complex **2**

[Zn(CH_3OH)$_3$(oFBPDC)]

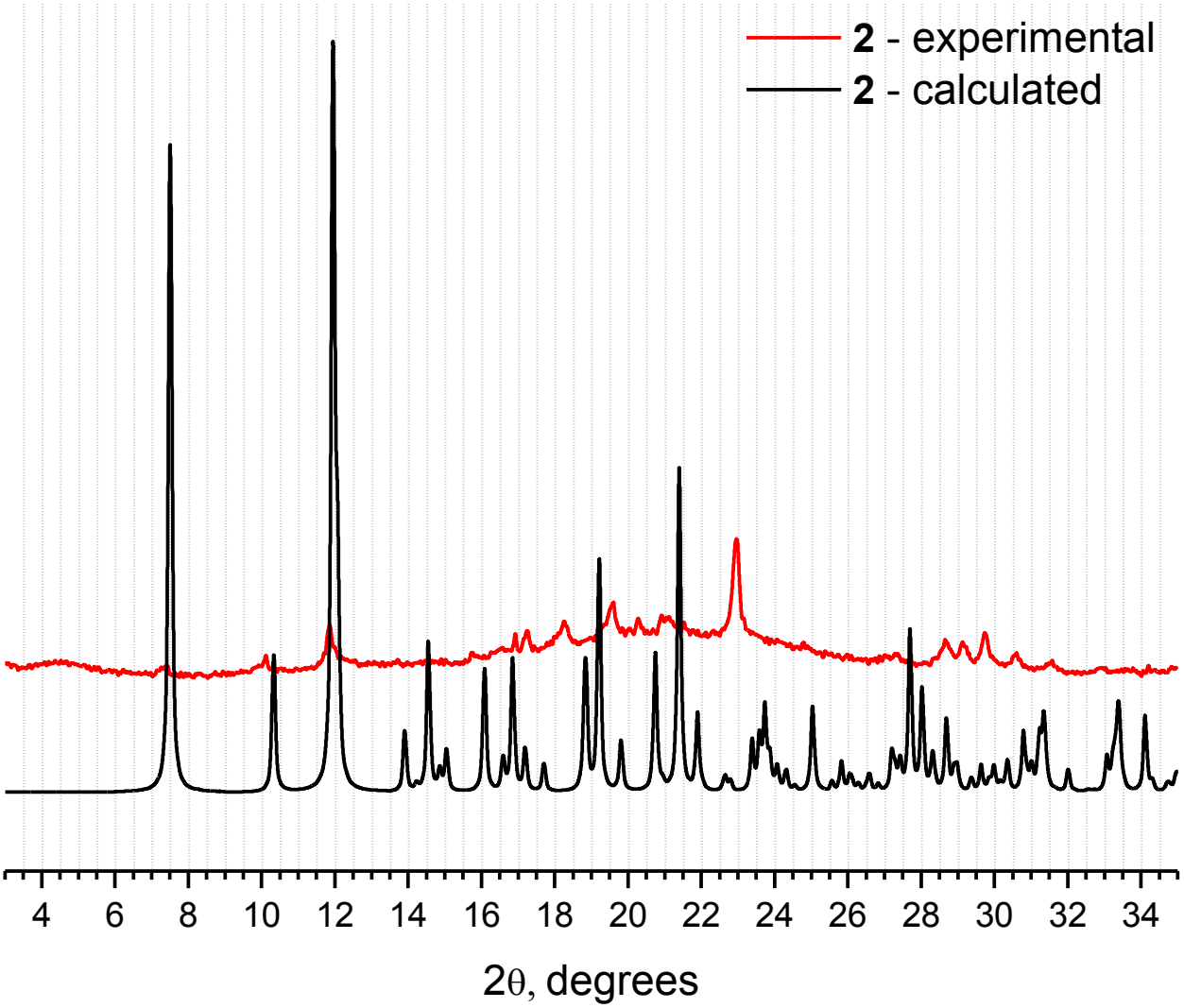

Fig. S20. Experimental after removal from mother liquor (red line) and calculated (black line) PXRD patterns of complex **2**. Absence of some reflections indicates that the sample loses original crystal structure.

Complex **3**

$[Zn_2(H_2O)_{1.5}(thf)_{1.5}(oFBPDC)_2]\cdot 3.5H_2O\cdot 2.5THF$

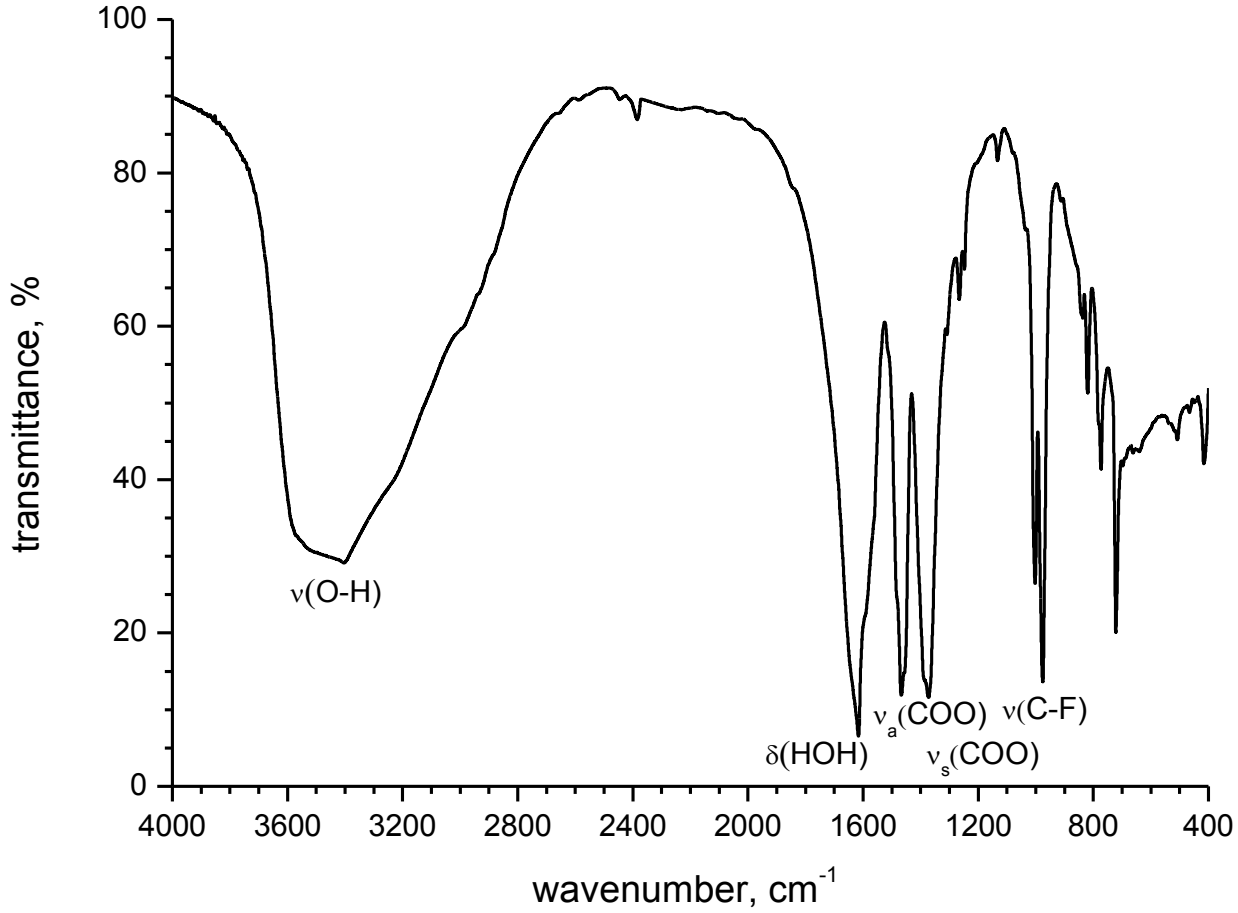

Fig. S21. The FT-IR spectrum of complex **3**.

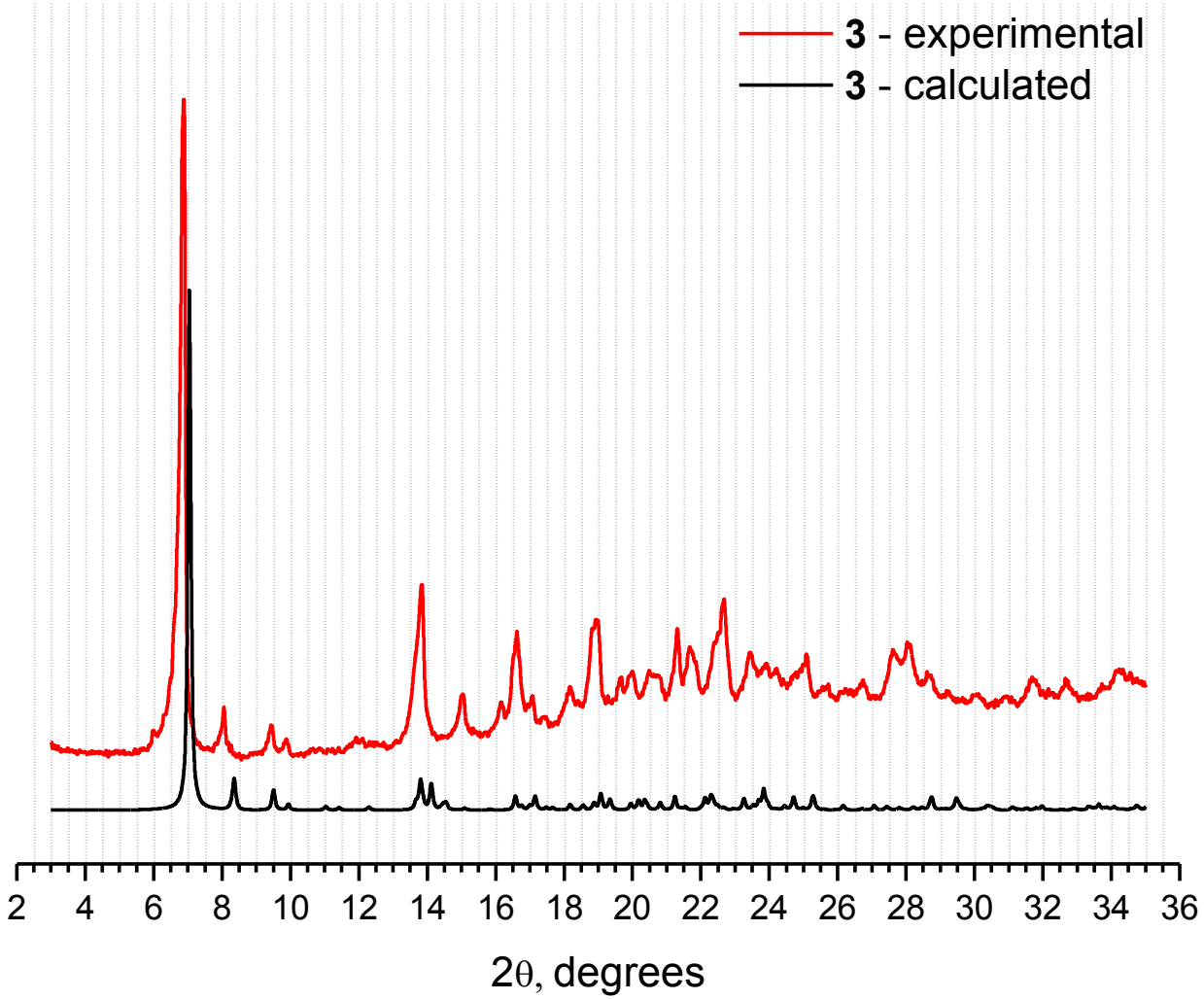

Fig. S22. Experimental (red line) and calculated (black line) PXRD patterns of complex **3**.

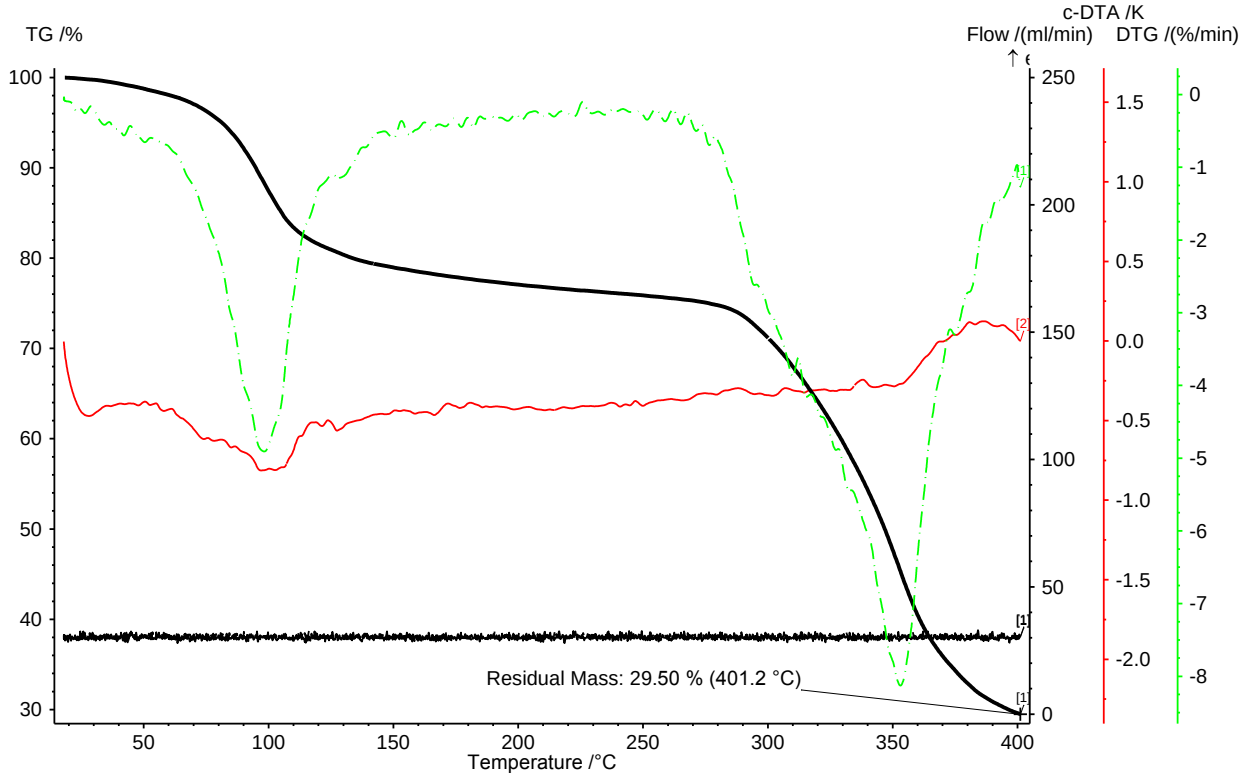

Fig. S23. TG curve of complex **3**.

Complex **4**

$[Zn_2(dabco)(oFBPDC)_2]\cdot 4.5CH_3OH$

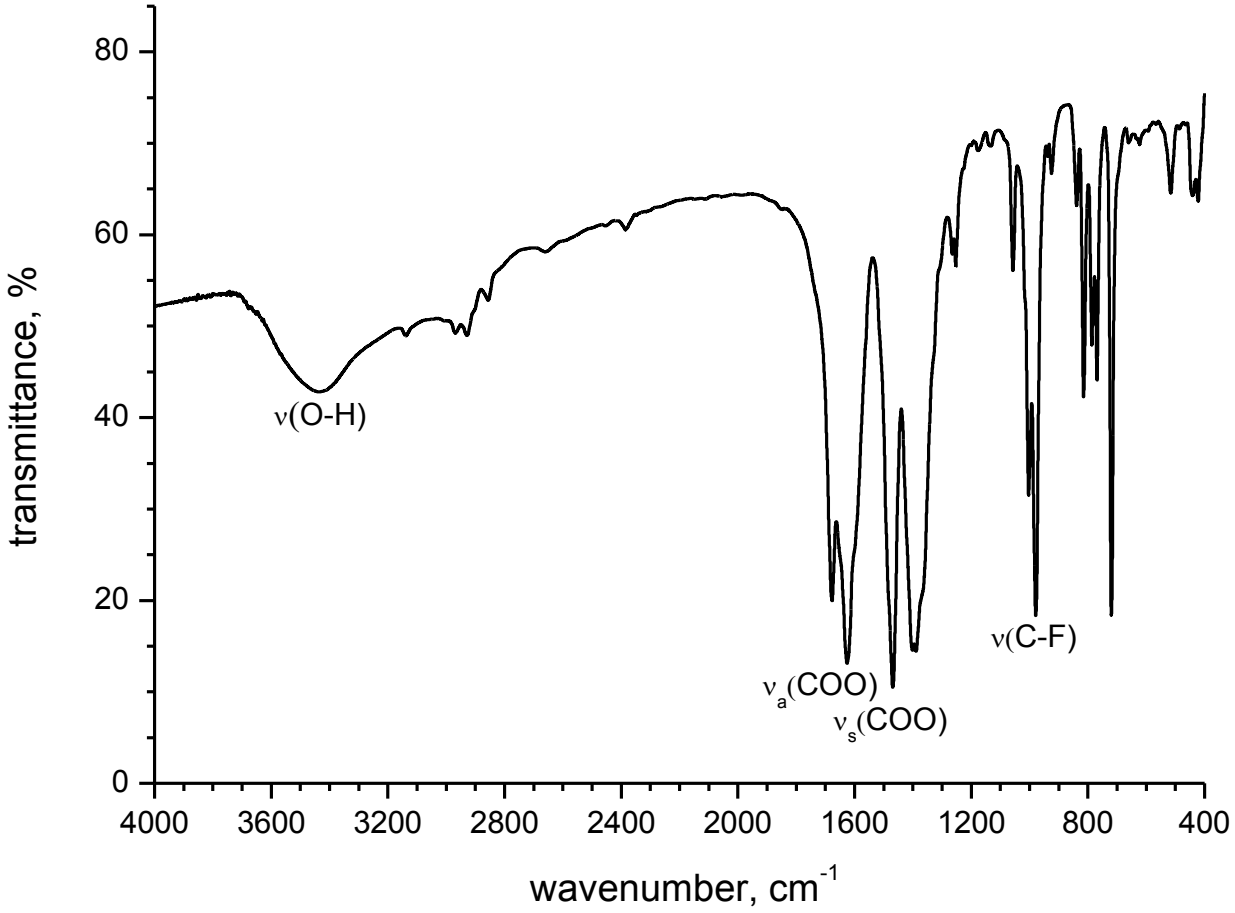

Fig. S24. The FT-IR spectrum of complex **4**.

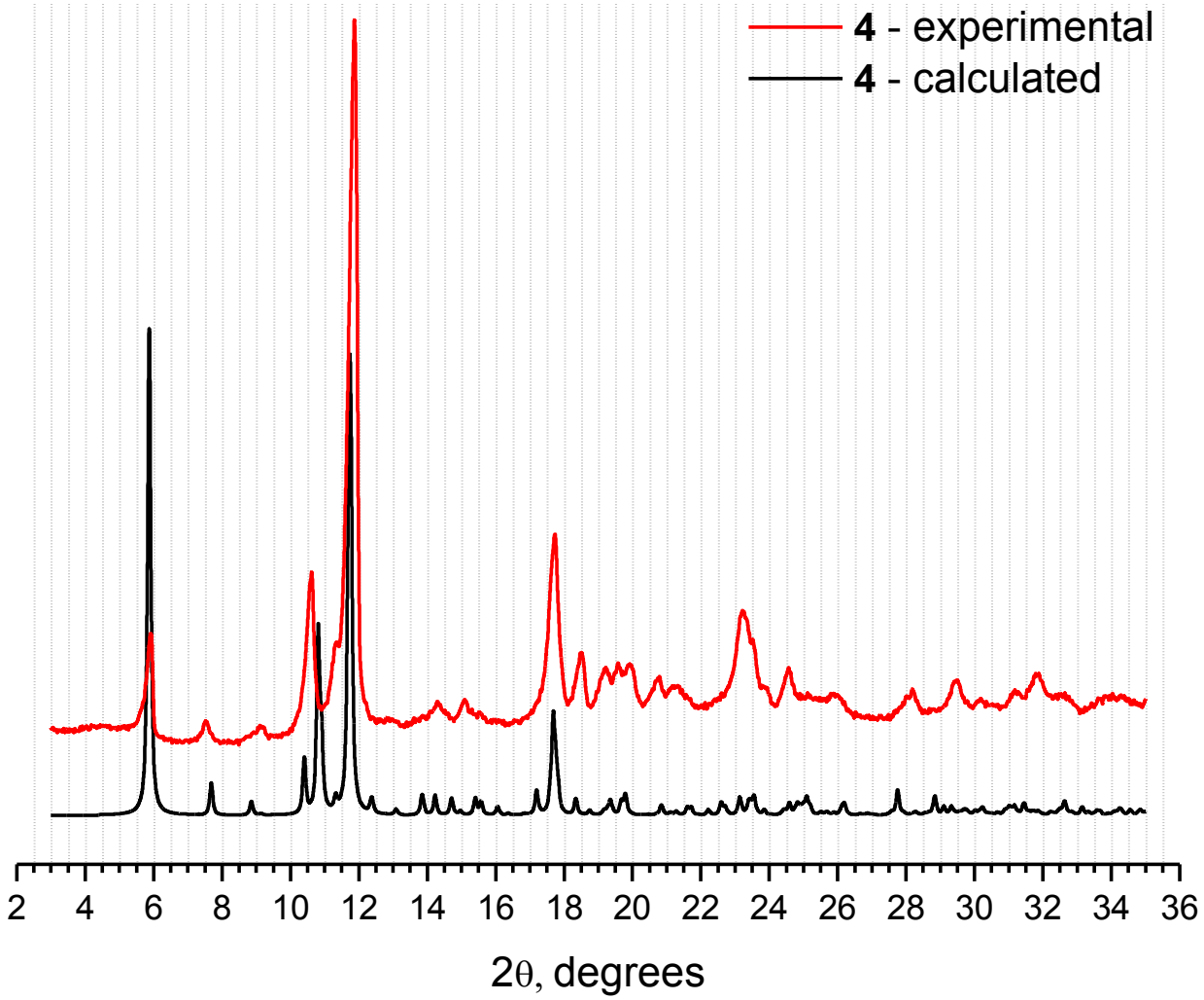

Fig. S25. Experimental (red line) and calculated (black line) PXRD patterns of complex **4**.

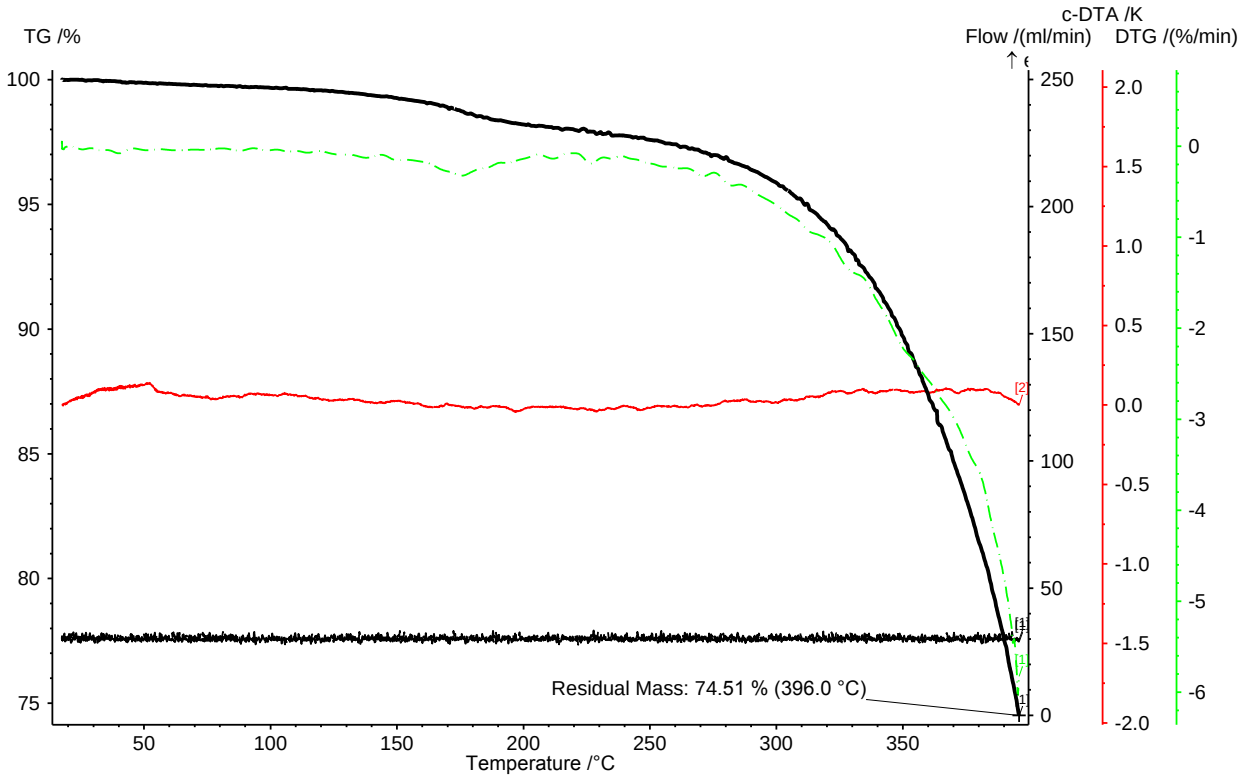

Fig. S26. TG curve of complex **4**.

Complex **5**

$(H_2bpy)[Zn_2(bpy)(oFBPDC)_3]$

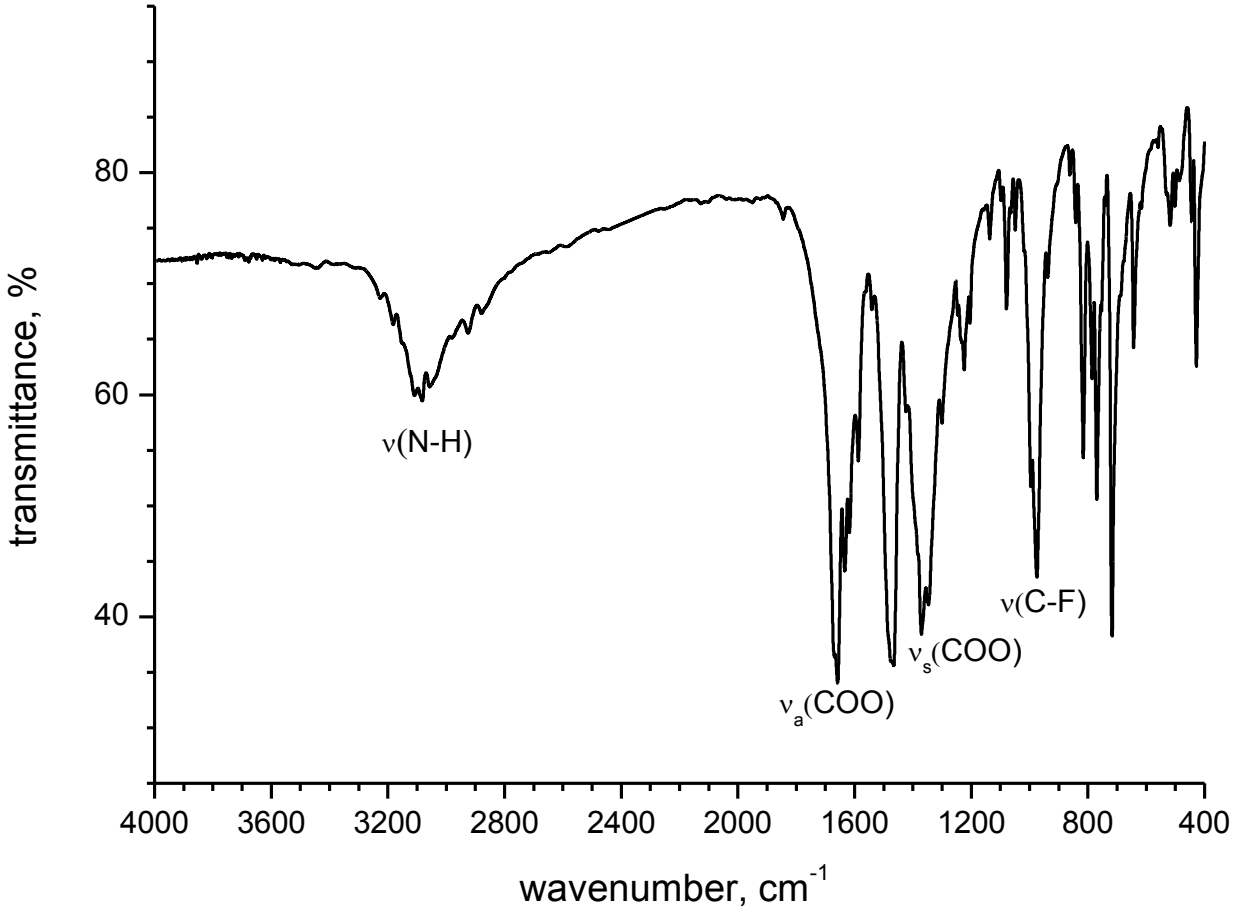

Fig. S27. The FT-IR spectrum of complex **5**.

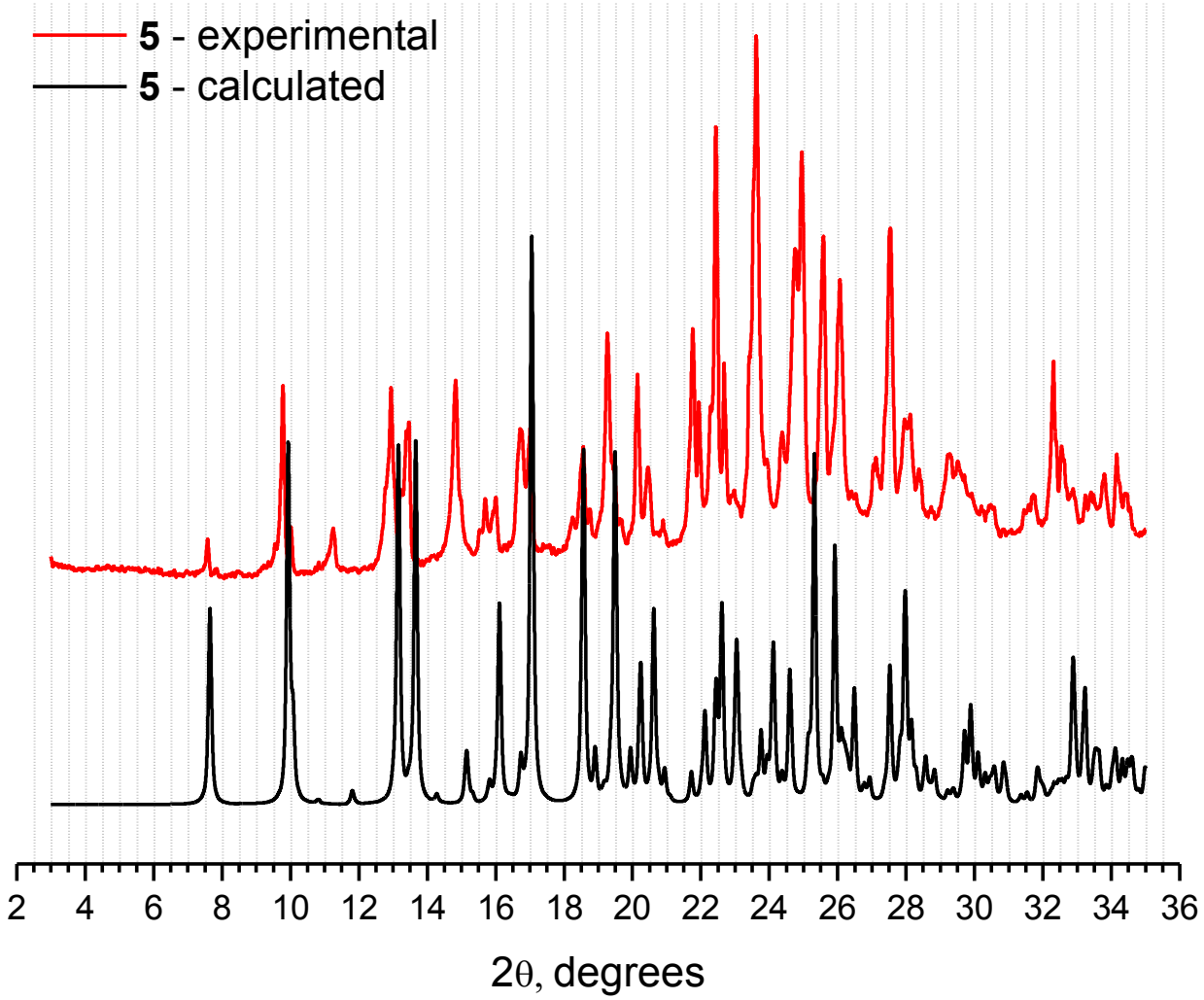

Fig. S28. Experimental (red line) and calculated (black line) PXRD patterns of complex **5**.

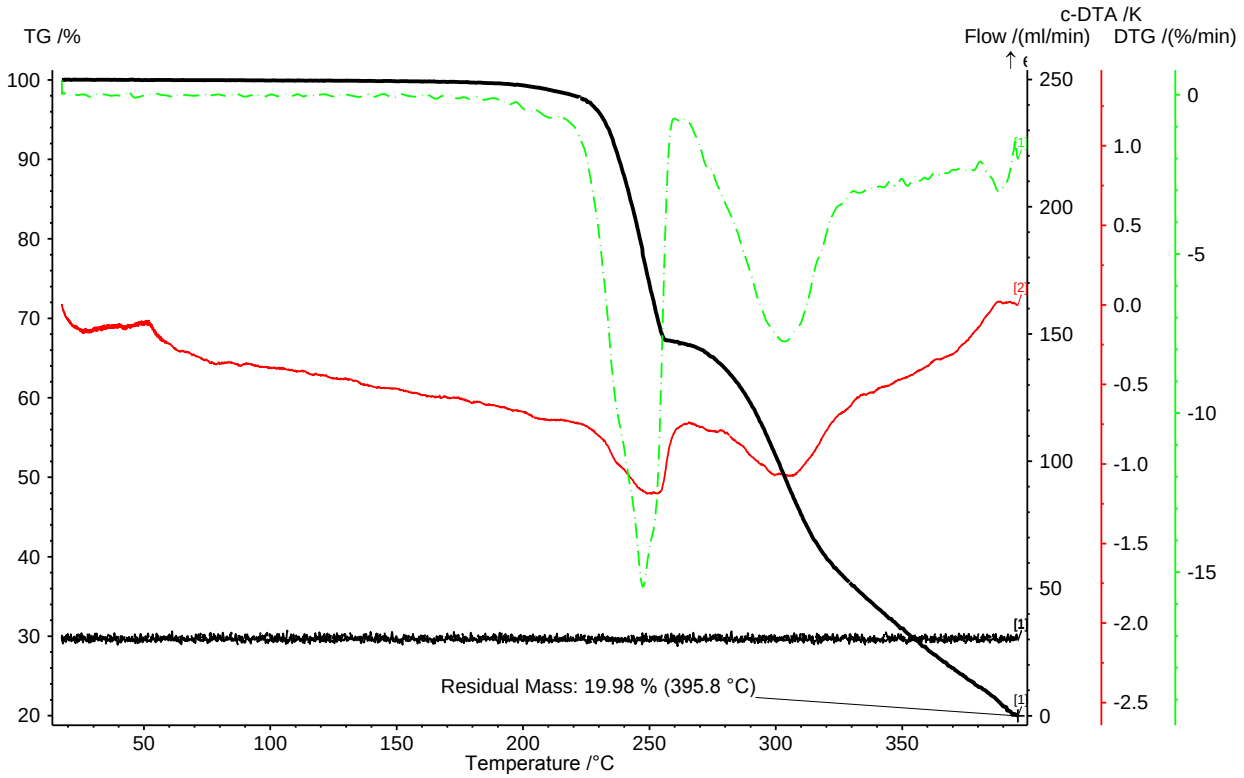

Fig. S29. TG curve of complex **5**.

Complex **6**

$[Zn(CH_3OH)_3(ur)(oFBPDC)]$

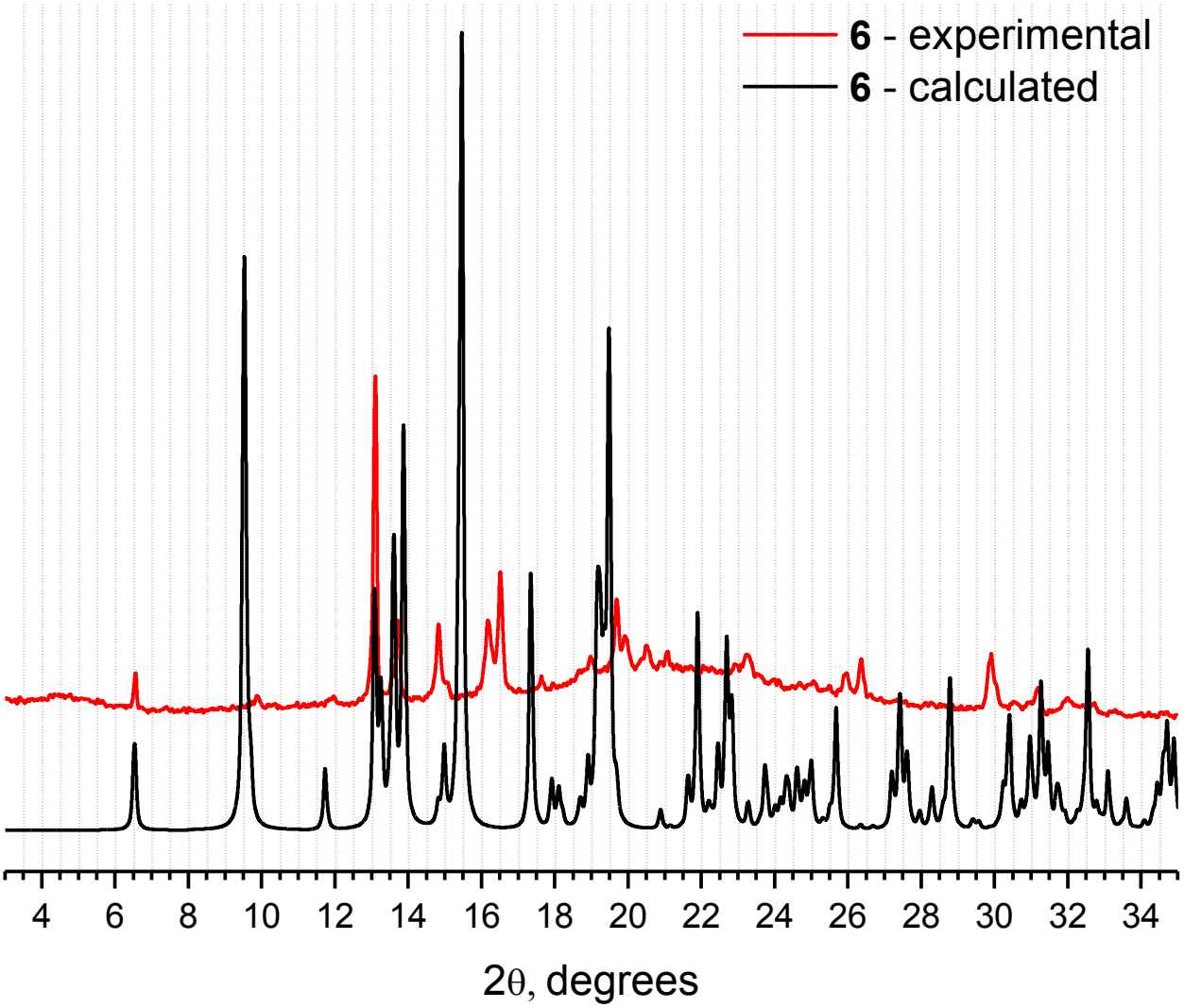

Fig. S30. Experimental after removal from mother liquor (red line) and calculated (black line) PXRD patterns of complex **6**. Discrepancy between calculated and experimental patterns proves that the complex **6** is stable only in the mother liquor.

Stability of complex 4

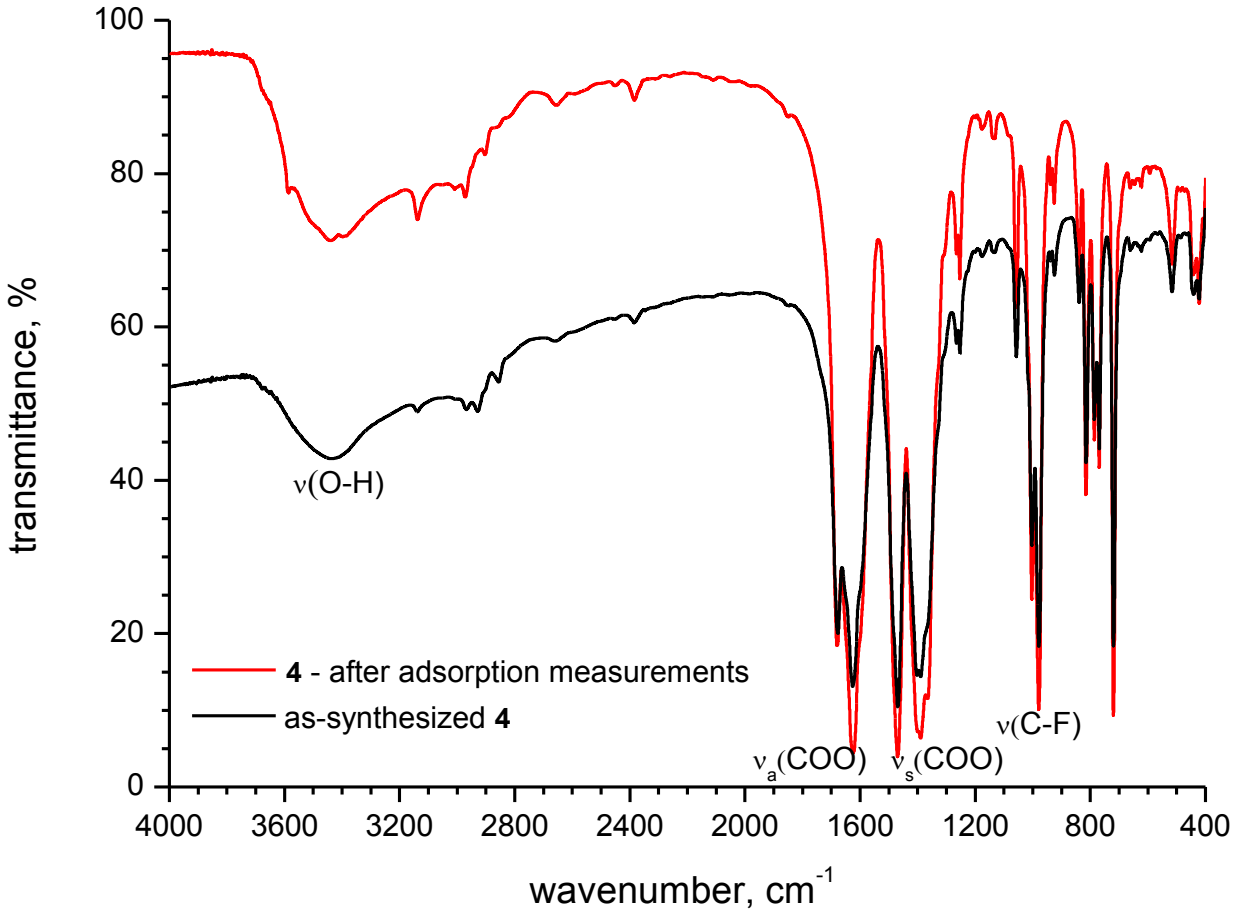

Fig. S31. FT-IR spectra of as-synthesized complex **4** (black curve) and that after all gas and vapor adsorption measurements (red curve).

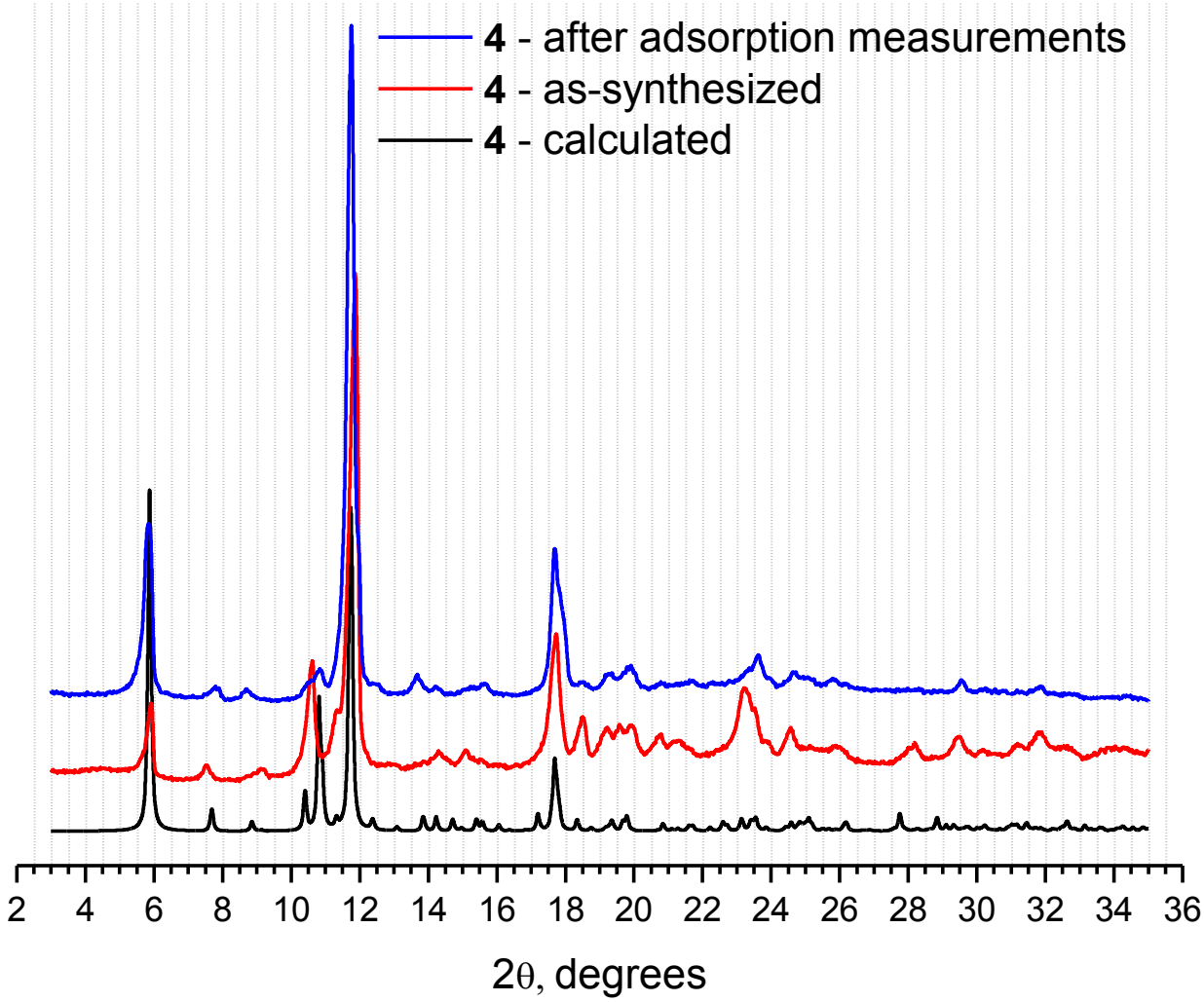

Fig. S32. PXRD patterns of as-synthesized complex **4** (red curve) and that after all gas and vapor adsorption measurements (blue curve).

Adsorption of gases and vapors

Fit of gas adsorption isotherms

For different calculations, CH_4, CO_2 and N_2 adsorption isotherms at 273 K and 298 K were fitted by appropriate model. The list of models, final sets of fitted parameters as well as graphs with fitted isotherms are given below.

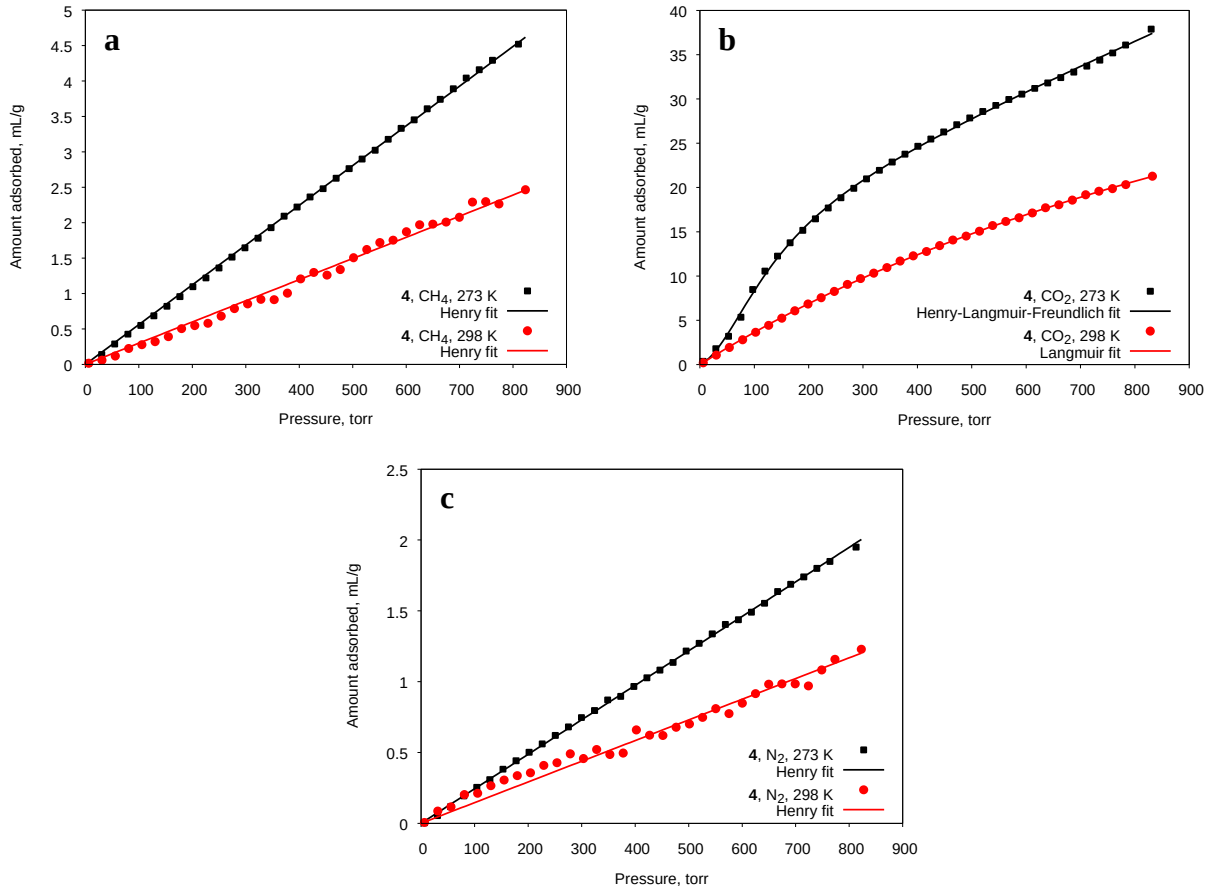

Fig. S33. Fitted isotherms of adsorption on **4** at 273 K and 298 K: a) CH_4, b) CO_2, c) N_2.

Methane

Henry model was used for fitting adsorption isotherms at 273 and 298 K.

Henry equation: $n = K_H \cdot p$

Table S7. Fitted isotherm parameters for methane adsorption.

Final set of parameters		Asymptotic Standard error	
273 K			
K_H	$5.611 \cdot 10^{-3}$	$\pm 9 \cdot 10^{-6}$	0.2%
298 K			
K_H	$2.988 \cdot 10^{-3}$	$\pm 2.5 \cdot 10^{-5}$	0.8%

Carbon dioxide

The sum of **Henry** and **Langmuir-Freundlich** equation was used for fitting isotherm at 273 K while isotherm at 298 K was well fitted by **Langmuir** model.

The sum of Henry and Langmuir-Freundlich equations: $n = k \cdot p + \frac{wbp^{1/t}}{1 + bp^{1/t}}$

Langmuir equation: $n = \frac{wbp}{1 + bp}$

Table S8. Fitted isotherm parameters for carbon dioxide adsorption.

Final set of parameters		Asymptotic Standard error	
273 K			
k	0.0271	$\pm 8 \cdot 10^{-4}$	3.1%
w	15.3	± 0.7	4.7%
b	$8 \cdot 10^{-5}$	$\pm 4 \cdot 10^{-5}$	45%
t	0.518	± 0.029	5.5%
298 K			
w	62.6	± 0.6	1.0%
b	$6.18 \cdot 10^{-4}$	$\pm 8 \cdot 10^{-6}$	1.4%

Nitrogen

Henry model was used for fitting adsorption isotherms at 273 and 298 K.

Henry equation: $n = K_H \cdot p$

Table S9. Fitted isotherm parameters for methane adsorption.

Final set of parameters		Asymptotic Standard error	
273 K			
K_H	$2.435 \cdot 10^{-3}$	$\pm 5 \cdot 10^{-6}$	0.2%
298 K			
K_H	$1.460 \cdot 10^{-3}$	$\pm 1.9 \cdot 10^{-5}$	1.3%

Fit of vapor adsorption isotherms

In general, fitting of vapor adsorption isotherms is more complicated task than fitting of gas adsorption isotherms. A lot of physical and empirical models have been tried. The most appropriate model found is the sum of Henry and Langmuir-Freundlich equations for both benzene and cyclohexane adsorption isotherms at both temperatures of 288 K and 293 K.

The sum of Henry and Langmuir-Freundlich equations: $n = k \cdot p + \frac{wbp^{1/t}}{1 + bp^{1/t}}$

Moreover, in opposite to gas adsorption, the Henry item of the sum is responsible for the ending part of isotherm while in gas sorption Henry equation usually describes well the initial part of isotherms. As a result, parameters were found with relatively large errors. Nevertheless, the calculated isotherms are in a good agreement with measured ones.

Table S10. Fitted isotherm parameters for benzene adsorption.

Final set of parameters		Asymptotic Standard error	
288 K			
k	0.099	±0.019	19.1%
w	37.14	±0.44	1.2%
b	29.6	±5.1	17.1%
t	0.466	±0.020	4.4%
293 K			
k	0.099	±0.014	13.9%
w	36.61	±0.33	0.9%
b	8.19	±0.73	8.9%
t	0.475	±0.016	3.3%

Table S11. Fitted isotherm parameters for cyclohexane adsorption.

Final set of parameters		**Asymptotic Standard error**	
288 K			
k	0.157	±0.018	12%
w	13.77	±0.17	1.2%
b	$7.6 \cdot 10^3$	$\pm 3.9 \cdot 10^3$	52%
t	0.081	±0.004	5.6%
293 K			
k	0.132	±0.022	17%
w	14.10	±0.26	1.8%
b	1.98	±0.20	10%
t	0.122	±0.010	7.9%

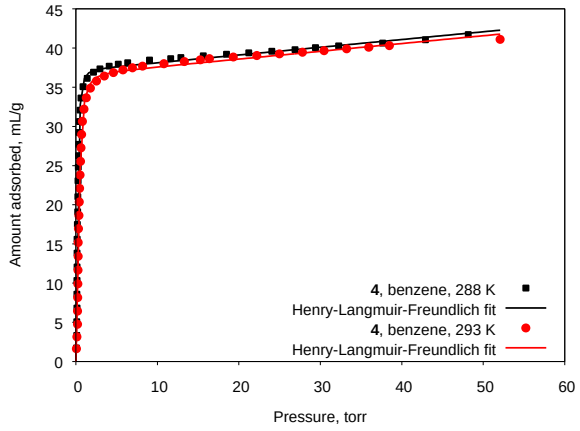

a)

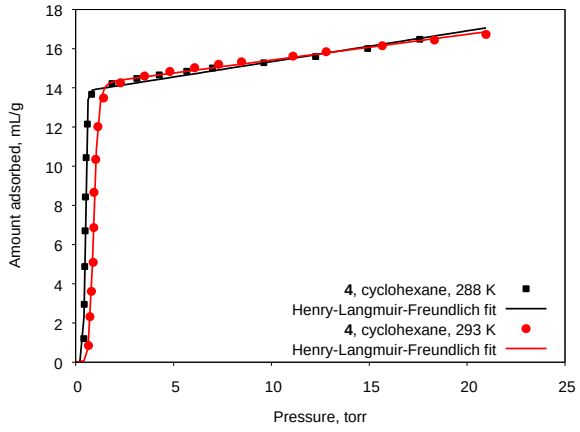

b)

Fig. S34. Fitted vapour adsorption isotherms on **4** at 288 K and 293 K for a) benzene, b) cyclohexane.

Fit of adsorption isotherms by virial equation and isosteric heats of adsorption

Adsorption isotherms were fitted with the virial equation:

$$p(n,T) = \ln n + \frac{1}{T}\sum_i A_i n^i + \sum_j B_j n^j$$

The final sets of parameters are given in Table S12 while fitted graphs represented in Fig 35.

Table S12. Virial coefficients for CH_4, CO_2 and N_2 adsorption isotherms at 273 K and 298 K on **4** and corresponding heat of adsorption at zero coverage.

Coefficient	CH_4	CO_2	N_2
A_0	−2155±90	−2809±92	−1201±192
A_1	—	96±8	—
B_0	9.6±0.3	9.2±0.3	7.0±0.7
$\Delta H(0)$, kJ/mol	17.9	23.4	9.99

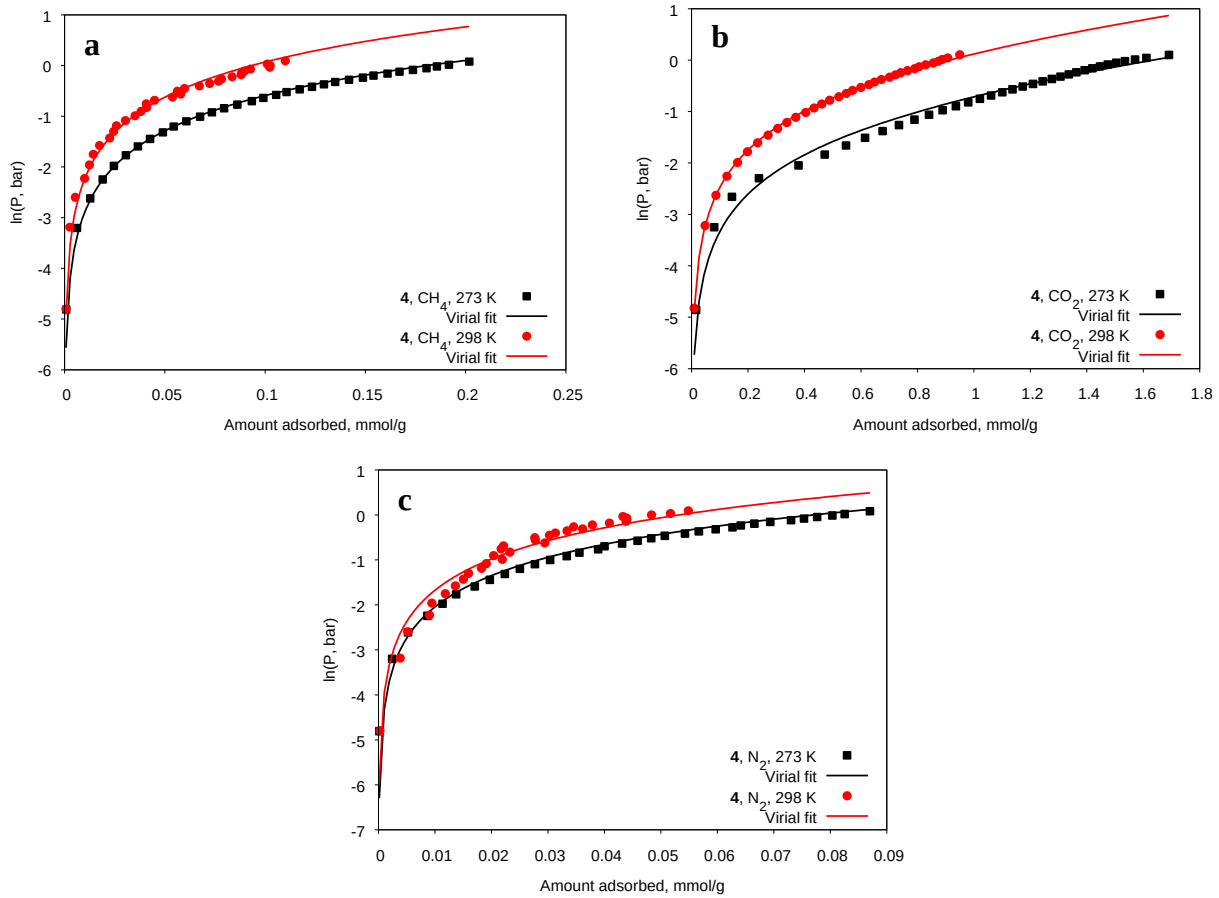

Fig. S35. Gas adsorption isotherms fitted by virial equation: a) CH_4, b) CO_2, c) N_2.

Henry constants

Henry constants were calculated by means of virial equation:

$$K_h = \exp\left[\frac{A_0}{T} + B_0\right]$$

Founded Henry constants for gas adsorption isotherms are summarized in Table S13.

Table S13. Calculated Henry constants for gas adsorption isotherms at 273 K and 298 K.

Units	**273 K**			**298 K**		
	CH_4	**CO_2**	**N_2**	**CH_4**	**CO_2**	**N_2**
mmol·g^{-1}·bar^{-1}	0.1452	2.638	0.07011	0.07922	1.089	0.04946

Selectivity calculations

Selectivity factors were evaluated by three commonly used methods:

(i) As the molar ratio of the adsorption quantities at the relevant partial pressures of the gases:

$$S = \frac{n_1 / n_2}{p_1 / p_2},$$

where S is the selectivity factor, n_i represents the adsorbed amount of component i, and p_i represents the partial pressure of component i.

(ii) As a ratio of Henry constants which corresponds to the slope of the adsorption isotherm at very low partial pressures:

$$S = \frac{K_{H1}}{K_{H2}}$$

(iii) By ideal adsorbed solution theory (IAST). The relationship between P, y_i and x_i (P — the total pressure of the gas phase, y_i — mole fraction of the i-component in the gas phase, x_i — mole fraction of the i-component in the absorbed state) is defined according to the IAST[1]:

$$\int_{p=0}^{p=\frac{Py_1}{x_1}} n_1(p)\,d\ln p = \int_{p=0}^{p=\frac{Py_2}{x_2}} n_2(p)\,d\ln p$$

In this case, the selectivity factors were determined as:

$$S = \frac{y_2 / x_2}{y_1 / x_1} = \frac{x_1(1 - y_1)}{y_1(1 - x_1)}$$

Heats of Adsorption

Heats of adsorption were calculated based on virial fitting using the equation:

$$\Delta H \left[\text{kJ/mol} \right] = -\frac{R}{1000}\sum_i A_i n^i$$

The values of isosteric heat of gas adsorption at zero coverage are summarized in Table S12.

Water adsorption

Table S14. Summary of textural and water sorption properties for MOFs with the comparable surface area as for **4**.

MOF	Pore diameter, nm	S_{BET}, m^2/g	Pore Volume, cm^3/g	α	Water Uptake, g/g	Ref.
CAU-6	0.5/1.0	625	0.25	0.15	0.32	2
CAU-6	0.5/1.0	760	0.34	0.05	0.3	3
CAU-10	0.7	635	0.25	0.17	0.31	4
CAU-10	0.7	600	0.26	0.15	0.3	3
UiO-66-fumarate	0.5/0.7	690	0.27	0.1	0.28	3
SIM-1	0.6	470	0.23	0.25	0.12	5
4	0.7	441	0.22	0.59	0.02	This work

References

1 A. L. Myers and J. M. Prausnitz, *AIChE J.*, 1965, **11**, 121–127.

2 H. Reinsch, B. Marszalek, J. Wack, J. Senker, B. Gil and N. Stock, *Chem. Commun.*, 2012, **48**, 9486–9488.

3 H. Furukawa, F. Gándara, Y.-B. Zhang, J. Jiang, W. L. Queen, M. R. Hudson and O. M. Yaghi, *J. Am. Chem. Soc.*, 2014, **136**, 4369–4381.

4 H. Reinsch, M. A. van der Veen, B. Gil, B. Marszalek, T. Verbiest, D. de Vos and N. Stock, *Chem. Mater.*, 2013, **25**, 17–26.

5 J. Canivet, J. Bonnefoy, C. Daniel, A. Legrand, B. Coasne and D. Farrusseng, *New J. Chem.*, 2014, **38**, 3102–3111.